Chapter 2
Kinetic Features of Three-Dimensional Free-Radical Polymerization

Abstract Key results of systematic exploration into three-dimensional free-radical polymerization (TFRP) in blocks, solutions, and films carried out by the authors are described in Chap. 2. An interpretation of TFRP kinetic features takes the microheterogeneous mechanics of polymerization into account. The factors determining the effective reactivity of unsaturated oligomers (allyl and vinyl types) under different conditions and at various TFRP stages were identified. All this enabled the authors to create a scientific basis of control over TFRP needed to produce different-purpose polymeric materials.

The main kinetic features of TFRP were determined in a series of systematic studies conducted by the authors with the use of oligo(acrylates) starting in 1960 [1–5]. Oligo(acrylates) were found to be very convenient oligomers for such experiments because their synthesis method enables us to vary, as targets, chemical composition and oligomer block size in a wide range, with the end methacrylate or acrylate groups able to polymerize being invariable [1, 3].

Processes of TFRP for polyunsaturated oligomers (monomers) of various structures have a similar development pattern. At the initial stage (in nonstructured reaction medium), the polymerization rate W_0 remains constant in a rather narrow range of conversions, $0 < C < 3 - 4\%$; then, in the period of polymerization auto-acceleration, it increases with growing C, and then with conversion $C_{\max}$, it becomes maximal $W_{\max}$. Subsequently, polymerization auto-deceleration takes place with complete TFRP process termination when limit conversion $C_{\lim} < 100\%$. During periods of auto-acceleration and auto-deceleration, polymerization proceeds in a structured reaction medium. The analysis of main kinetic TFRP features requires identifying factors determining the effective reactivity of oligomers (monomers) at each consecutive stage of the process as well as in different TFRP conditions (in the presence of inhibitors, in solutions, and in films).

G.V. Korolev, M.M. Mogilevich, *Three-Dimensional Free-Radical Polymerization*,
DOI 10.1007/978-3-540-87567-3_2,

2.1 Kinetic Features of Individual Stages of Polymerization

2.1.1 Initial Stage of Polymerization

Studying the initial stage of polymerization (up to a gel point, in unstructured reaction medium) enables identifying those oligomer-inherent kinetic parameters that at later stages are masked by formation of cross-linked polymer.

2.1.1.1 Influence of Oligomer Viscosity on Initial Polymerization Rate

Table 2.1 contains data showing correlation of initial polymerization rate W_0, characterizing oligomer reactivity, and macroscopic viscosity of oligomers η [6, 7].

W_0 increases with conversions $C \to 0$ as the viscosity grows. In its turn, reaction medium viscosity for small conversions is regulated by intensity of intermolecular interactions (IMI) of molecules of initial oligomers. Molecules have centers of strong IMI able to form dipole–dipole and other labile intermolecular bonds. Oligomer molecules (Table 2.1) have strong IMI centers that are systematically varying from two ester groups with intermolecular interaction energy $E_{IMI} = 18.4\,kJ/mol$ for tEGdMA to six ester and two phenyl groups with $E_{IMI} = 31.8\,kJ/mol$ for oligomer MDP-2 [8]. Associated methylene groups $(—CH_2—)_n$ may also serve as strong IMI centers. Each of these groups is characterized by very weak dispersion interactions (in case of $n \geq 4$ these groups enter into IMI with $E_{IMI} > 17\,kJ/mol$ comparable with energy of hydrogen bonds) [9]. Oligomer viscosity grows concurrently with an increase in the number of IMI centers and IMI energy.

Table 2.1 Initial polymerization rates of (oligo)acrylates W_0 in block and solution at 50°C

Oligomer	Oligomer repeating unit	Kinematic viscosity ν at 20°C, mm^2/s	$W_0 \times 10^2$, min^{-1}		
			In block	In solution, with oligomer **ID(PD)$_2$DI** content, %	
				50	75
tEGdMA	**MTM**	10	3.0	5.0	8.0
MDA	**MDADM**	55	3.0	–	7.5
MDP-1	**MDPDM**	60	4.0	4.3	8.0
MBP-1	**MBPBM**	115	5.0	6.0	8.0
MDP-2	**M(DP)$_2$DM**	1000	17.5	14.0	–

Note 1. Notation conventions for Tables 2.1, 2.4, and 2.5 only: **M**, **A**, **I**, **P**, residues of methacryl, adipine, isobutyric, and *ortho*-phthalic acids, respectively; **D**, **T**, and **B**, residues of diethylene glycol, triethylene glycol, and tetramethylene glycol, respectively.
Note 2. **I[DP]$_2$DI** with $\nu = 900\,mm^2/s$ at 20°C: initiator, dicyclohexylpercarbonate 0.5% (by weight), conversion $C \to 0$.

Dependence $W_0 = f(\eta)$ is sufficiently universal for oligo(acrylates) polymerization and trivial in terms of its physical sense. Indeed, W_0 is a function of the following kinetic parameters:

$$W_0 = \frac{k_{\text{pr}}}{k_{\text{ter}}^{1/2}} \cdot [M] \cdot W_i^{1/2} \tag{2.1}$$

where W_i = initiation rate; k_{pr} and k_{ter} = constants of chain propagation rate and chain termination rate; and [M] = oligo(acrylates) concentration.

Studies were conducted under conditions that were similar in terms of W_i and [M]: reduced polymerization rates $W_0/[\text{M}]$ of different oligomers with equal concentrations of one and the same initiator, with similar temperature, and for conversion $C \to 0$ were compared. Chain termination constant k_{ter} [10, 11] should be a parameter that is the most sensitive to viscosity variation in the reaction medium. The authors have found considerable decrease of k_{ter} as the viscosity grows, under the conditions of diffusion control over reaction of quadratic chain termination. The termination in case of TFRP (even with $C \to 0$) is limited by diffusion, while the latter is limited by viscosity. The higher is the viscosity, the lower is the value of effective constant k_{ter} and, therefore, the higher is W_0.

2.1.1.2 Influence of Regular Associates of Oligomer (Monomer) upon Initial Polymerization Rate

Kinetic Anomalies of Oligo(Acrylate) Polymerization: Role of Regular Associates (Hypothesis)

Dependence of initial polymerization rate W_0 on oligo(acrylates) nature comprises not only viscosity influence. In some cases at the initial TFRP stage, abnormal reactivity of oligomers was observed, and this reactivity was interpreted based on the assumption implying the existence of regular kinetically active associates in liquid oligo(acrylates).

For example, when measuring values of chain propagation rate constant k_{pr} and chain termination rate constant k_{ter} during polymerization of (alkylene glycol) dimethyl acrylates with different sizes of hydrocarbon chain $(\text{—CH}_2\text{—})_n$ for conversions $C \to 0$, an abnormally high value of k_{pr} was found, which increased threefold as n increased from 4 to 10 (Table 2.2) [12]. Also, the value of k_{pr} declines to normal ($k_{\text{pr}} \approx 3001 \cdot \text{mol}^{-1} \cdot \text{s}^{-1}$ at 25°C for methacrylates [10, 13, 14]) with increasing degree of conversion. The size of the hydrocarbon fragment of (alkylene glycol) dimethyl acrylate molecules does not influence the electron density distribution of double bonds and cannot alter their reactive capacity; hence, the values of k_{pr} of alkyl (meth)acrylates, differing in terms of size of their alkyl fragments, are quite close [10, 13, 14].

In another case, during polymerization of hexamethacrylate (bis-pentaerythrite) adipate (hMA-PeA) [15], an abnormal influence of viscosity upon initial

Table 2.2 Values of chain propagation rate constant (k_{pr}) and chain termination rate constant (k_{ter}) (25°C) for polymerization of alkylene glycol dimethyl acrylates at different conversions

Conversion, %	dMABDO		dMAHDO		dMADDO	
	K_{pr}, l/(mol·s)	k_{ter}, l/(mol·s)	k_{pr}, l/(mol·s)	k_{ter}, l/(mol·s)	k_{pr}, l/(mol·s)	k_{ter}, l/(mol·s)
≈0	≈600	$\approx 8 \times 10^5$	≈1200	$\approx 6.2 \times 10^5$	≈1880	$\approx 4.2 \times 10^5$
2.5	173	7.8×10^4	690	2.1×10^5	1660	1.9×10^5
5	112	2.3×10^4	245	3.6×10^4	1400	1.54×10^5
10	63	5.7×10^3	102	8.6×10^3	1900	9.6×10^4
15	41.5	2.5×10^3	89	5.8×10^3	1880	6.7×10^4
20	33	1.8×10^3	59	3.1×10^3	1700	5.4×10^4
30	17	8.3×10^2	26	1.3×10^3	840	2.5×10^4
40	3.4	1.5×10^2	9.5	4.3×10^2	196	5.9×10^3
50	–	–	–	–	24	6.5×10^2

Note 1. dMABDO, dimethylacrylate-1,4-butandiole; dMAHDO, dimethylacrylate-1,6-hexandiole; dMADDO, dimethylacrylate-1,10-decandiole.
Note 2. Photoinitiator, benzophenone; $W_i = 7 \times 10^{-9}$mol/(l·s).

polymerization rate W_0 was found: viscosity decrease after dilution by inert solvents resulted not in the decline of W_0 but, on the contrary, in its increase (Fig. 2.1).

These anomalies suggested the presence of another, specific feature of TFRP for low-degree conversions; namely, influence on polymerization kinetics of regular associates that are sufficiently stable at polymerization temperature and that are formed in initial oligo(acrylates) [16, 17].

Indeed, oligo(acrylates) homo-polymerization in thin films in the air [18] is indicative of oligo(acrylate) ability to form structurally ordered regions (associates) with a long period of structural relaxation even at 65°–80°C. For low-degree

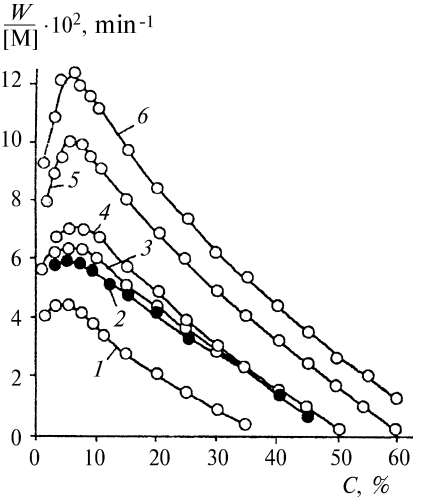

Fig. 2.1 Influence of solvents on hMA-PeA polymerization rate at 65°C: *1*, *4*, toluene; *2*, butyl acetate; *3*, chlorobenzene; *5*, dimethyl formamide; *6,* formamide. Solvent concentration, % (by weight): *1*, 6; *2–6*, 24; benzoyl peroxide concentration, 1.5% (by weight)

conversions under the conditions when O_2 diffusion rate into the film from the air is much higher than its utilization rate for the copolymerization reaction of oligomer with oxygen $\sim M^{\bullet} + O_2 \rightarrow \sim MO_2^{\bullet}(1)$ and $\sim MO_2^{\bullet} + M \rightarrow \sim MOOM^{\bullet}(2)$, homopolymerization develops $\sim M^{\bullet} + M \rightarrow \sim MM^{\bullet}(3)$; hence, $W_3/W_2 = 5$–10. Under such conditions, normally reaction (1) should prevail over the competing reaction (3) because $k_1[O_2] > k_3[M]$. Possibly, the liquid oligomer structure is characterized by such perfect molecule packing in the associates that either diffusion coefficient or oxygen solubility (or both) drop dramatically as compared to conventional weakly associated liquids.

Further accumulation of polymer (as conversion increases) results in structural rearrangement and normal oxidative polymerization with formation of copolymer of oligomer with oxygen $(—M—O—O—)_n$ with composition 1:1.

Polyfunctional molecules of oligomers with strong IMI centers are characterized by ability to form physical associates, the lifetime τ_{ph} of which may go as high as those values that are comparable with characteristic time of polymer chain propagation time τ_{pr}. Obviously, if $\tau_{ph} > \tau_{pr}$ and the association degree of initial oligomer molecules is quite high, the polymer chain propagation proceeds in the associated reaction medium. In this case mutual orientation of molecules in the associate, if it is regular and characterized by correlation time $\tau_{cor} > \tau_{pr}$, can be either advantageous or disadvantageous for the polymer chain propagation reaction.

An abnormally high value of k_{pr} can be explained by the presence of regular associates with mutual orientation of molecules in the associate that is advantageous for polymerization reaction (preformed associate). Increase of W_0 with dilution presumes that mutual orientation of molecules in the associate is disadvantageous (anti-preformed associate). Breakage of such associates with increasing dilution degree provides increase of initial polymerization rates W_0.

A hypothesis about the presence of kinetically active associates in liquid oligo(acrylates) [15, 16] is based on the fundamental concepts of Academician N.N. Semenov regarding structures with mutual orientation of molecules that is advantageous for the polymerization process. These structures are responsible for abnormal polymerization acceleration of certain vinyl monomers at phase transition temperature "crystal → liquid" [19].

Thus, initial polymerization rate W_0 in nonstructured reaction medium (with $C \rightarrow 0$) is significantly influenced by the initial oligo(acrylates) nature for least by two reasons. First, the existence of fundamental reverse viscosity dependence of chain termination rate constant $k_{ter} = f(1/\eta)$ leads to direct dependence $W_0 = f(\eta)$. Second, presumably the existence of sufficiently stable regular associates in liquid oligo(acrylates) with the advantageous or, in contrast, disadvantageous location of oligomer molecules in associates leads to further propagation of the polymer chain.

Kinetic Anomalies of Polymerization of Higher Alkyl (Meth)Acrylates. Model of Regular Kinetically Active Associates

Kinetic anomalies of oligo(acrylates) polymerization, presumably related to the formation of regular associates, are especially clearly manifested in polymerization

of higher alkyl (meth)acrylates that could be considered as oligo(acrylates) models containing strong IMI centers in their molecules. Diphilic molecules of monomers with such structure can easily form regular associates of the micellar type, in which hydrophilic and hydrophobic fragments of molecules are segregated and mutually ordered in terms of their position and orientation [20]. An example of alkyl (meth)acrylates polymerization enabled us not only to prove the existence of preformed and anti-preformed associates and their influence on kinetics of polymerization processes but also to propose a quantitative model of polymer chain propagation in regular associates (model of regular kinetically active associates) [21, 22].

An exploration into the influence upon polymerization rate of small amounts (1–5% mol) of comonomers, which had a similar double bond but different size of alkyl substituent, as compared to the main comonomer, played a crucial role [21, 22]. The quite strong negative impact of such additives in the case of alkyl acrylate polymerization is interpreted based on the assumption that molecules of comonomers-additives are easily built in into preformed associates, but because of the difference of alkyl fragment size, they disturb positional and (or) orientation order of molecules in the associates. Due to the disadvantageous orientation of double bonds, molecules of comonomers-additives interrupt the growth of polymer chain (that develops within the preformed associate) because all reactions of free radical addition are strictly sterically regulated, which is indicated by very low values of the sterical factor: 10^{-5}–10^{-3} [23–25]. Based on these concepts, a calculation system [21, 22] was developed, which enables estimating the average number of molecules in a preformed associate of higher alkyl acrylates and ratio of chain propagation rate constants in the associate and outside it. This ratio was found to increase from 50 to 200 with an increase of n in a side alkyl fragment $CH_3(CH_2)_n$ from 4 to 12 and, correspondingly, with an enhancement of preformed associates stability.

The positive effect of small additives of congeneric monomers (observed in the case of higher alkyl methacrylate polymerization) is interpreted as an effect of anti-preformed associate breakage (or stability decline) by building in molecules with different positional or orientation order [21, 22, 26].

The model of regular kinetically active associates, although substantiated kinetically [21, 22, 26, 27], [28] p. 48, required direct experimental verification. However, as is well known, there are no direct experimental methods to study the structure and properties of associated structures of liquids [29–31]. At the same time, results of computer modeling for such structures by methods of molecular mechanics and molecular dynamics [32, 33] are not inferior to results of direct experiments in terms of reliability.

The authors conducted computer modeling of associate structures from methyl to cetyl esters in a homologous series of *n*-alkyl acrylates and *n*-alkyl (meth)acrylates [34] by computing spatial arrangement of associate molecules with minimal potential energy. Equilibrium conformations of associates of *n*-alkyl (meth)acrylates were calculated using the molecular mechanics method with parameterization of MM2 [32]. It was shown that higher *n*-alkyl acrylates and *n*-alkyl (meth)acrylates, starting from butyl esters, are able to form regular associates, in which ester molecules (their hydrocarbonic fragments, ester groups, and double bonds) are mutually ordered in terms of their location and orientation (Fig. 2.2). These regular associates

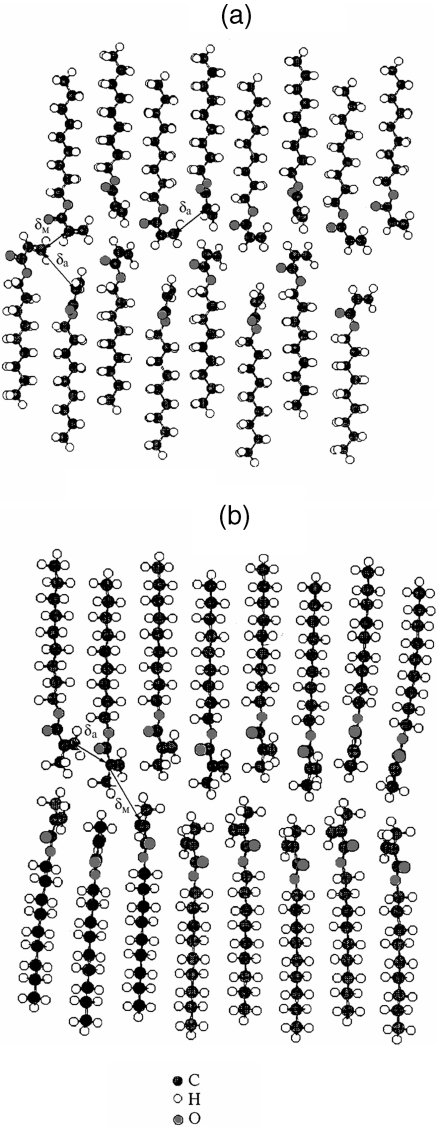

Fig. 2.2 Monomolecular section of the middle layer of regulate associate NonA (***a***) and NonMA (***b***)

can be identified with kinetically active associates that earlier were postulated for the interpretation of kinetic anomalies of radical polymerization of higher alkyl (meth)acrylates.

Double bonds in molecules of higher *n*-alkyl acrylates and *n*-alkyl (meth) acrylates are ordered both within the associates and in relationship to double bonds of neighboring associates [35]. In terms of intra-associate ordering of double bonds, the associates of nonyl acrylate (NonA), nonyl methacrylate (NonMA), and other *n*-alkyl acrylates and *n*-alkyl methacrylates are actually identical; in contrast, the

Table 2.3 Average distance between vinyl carbon atoms (δ) and mutual orientation angle of double bonds (θ) of neighboring molecules within associates (δ_a, θ_a) of alkyl (meth)acrylates and between associates (δ_{aa}, θ_{aa})

Associates	δ_a, Å	θ_a, degrees	δ_{aa}, Å	θ_{aa}, degrees
n-Alkyl acrylates				
BA	3.52	3	3.92	81
NonA	3.43	1	3.65	88
DDA	3.40	1	3.58	89
CEA	4.03	0	3.79	92
n-Alkyl (meth)acrylates				
BMA	3.48	3	6.75	177
NonMA	3.78	1	6.84	183
DDMA	3.58	1	6.24	182
CEMA	3.92	1	6.48	182

Note 1. Accuracy of determination of δ values in the models is ± 0.01 Å; θ values, ± 2.
Note 2. BA, butyl acrylate; NonA, nonyl acrylate; DDA, dodecyl acrylate; CEA, cetyl acrylate; BMA, butyl methacrylate; NonMA, nonyl methacrylate; DDMA, dodecyl methacrylate; CEMA, cetyl methacrylate.

inter-associate ordering of double bonds of molecules of *n*-alkyl acrylates and *n*-alkyl methacrylates, including NonA and NonMA, differs significantly (Fig. 2.2, Table 2.3).

One has grounds to believe that it is precisely these peculiarities of inter-associate ordering of double bonds of associated molecules that represent an advantageous factor for polymerization of higher *n*-alkyl acrylates and, in contrast, a disadvantageous factor for polymerization of higher *n*-alkyl (meth)acrylates. Probably these factors control the addition of polymer radicals to the double bonds of monomer molecules.

It has been established that incorporation of foreign matter molecules (e.g., small amount of comonomer) into associates not only alters the positional ordering of double bonds in sites of additive molecule localization, thus increasing the distance between carbon atoms of neighboring double bonds up to 5–9 Å, but also changes the molecular dynamics of all other molecules of the associate [35]. Modeling of the thermal motion of molecules in regular associates conducted using the molecular dynamics method [33] showed that inclusion of BA (BMA) molecules into a regular associate of NonA (NonMA) results in destabilization of associates (Fig. 2.3), shifting the associate $\rightleftarrows$ disassociate equilibrium in favor of nonassociated molecules of monomers.

For *n*-alkyl acrylates, it should result in the decrease of preformed associate concentration and corresponding decline of polymerization rate, while for *n*-alkyl (meth)acrylates it should result in the decrease of anti-preformed associates concentration and growth of polymerization rate.

Results of computer modeling of associative structures of higher alkyl(meth) acrylates permit us to interpret unambiguously kinetic anomalies of radical polymerization of these monomers for low conversions $C \to 0$ as kinetic manifestation of their regular associative structures that have such mutual location of double bonds

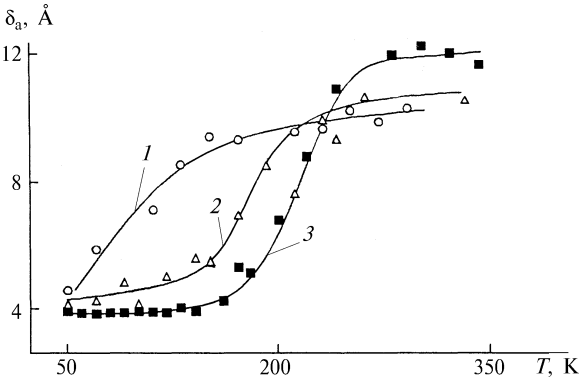

Fig. 2.3 Temperature dependencies of average distance between double bonds δ_a in various associates: *1*, BA; *2*, (NonA + BA); *3*, NonA

in regular associative structures, which is either advantageous (in case of alkyl acrylates) or disadvantageous [in case of alkyl (meth)acrylates] for polymer propagation reaction.

Thus, the hypothesis implying the existence of regular kinetically active associates [19] proposed to provide explanations for kinetic anomalies of polymerization of crystallizing monomers in the region of their phase transition [36–38] was then expanded in a high-temperature region far from phase transition temperatures by the discovery of kinetic anomalies of oligo(acrylates) polymerization [12, 15–18]. The model of regular kinetically active associates [21, 22] based on the afore-indicated hypothesis and substantiated with results of exploration into kinetic anomalies of polymerization of higher alkyl acrylates and alkyl (meth)acrylates [21, 22, 26] and with computer modeling of structure and temperature stability of associates of these monomers [34, 35] can be considered to be quite valid and reliable as applied to TFRP of polyunsaturated oligomers.

2.1.2 Stages of Auto-Acceleration and Auto-Deceleration

The TFRP auto-acceleration and auto-deceleration should be interpreted within the frames of diffusion kinetics: as diffusive mobility of reagents is hindered to a higher and higher degree, at first faster proceeding elementary acts (i.e., chain termination, k_{ter}) and then slower ones (i.e., chain propagation, k_{pr}) become diffusion controlled in the formed network structure of the reaction medium. Therefore, at first auto-acceleration develops because of the declining effective value of k_{ter}, and then auto-deceleration starts as a result of the decreasing effective value of k_{pr}.

One can draw an analogy with the widely known gel effect phenomenon appearing during conventional linear block polymerization of certain monomers [e.g., methyl methacrylate (MMA)], also resulting in the auto-acceleration – auto-deceleration sequence. Physical reasons are the same here: hindrance of diffusive mobility of reagents to the level where elementary reactions become diffusion controlled and effective values of their elementary rate constants begin diminishing

with a growth in diffusion hindrances. The only difference lies in the mechanism of diffusion mobility hindrance, which leads to considerable quantitative differences for TFRP, with the qualitative analogy being absolute.

In the case of linear polymerization, double bonds stay within monomers until the very end. Therefore, the diffusion control of processes with participation of monomer molecules (chain propagation) appears only at the very late stages of polymerization, when the polymer-monomer mix starts transiting into the glassy state. In the case of TFRP, initial molecules contain two or more double bonds. Addition of one of them to the growing network frame results in the appearance of "pendent" double bonds with extremely limited mobility (Fig. 2.4).

The mobility of double bonds of nonreacted oligomer molecules is probably also limited by incorporation of network fragments with uncompleted structure [39]. Therefore, not only termination, but also propagation, of the chain during TFRP becomes diffusion controlled even at low-degree conversions; this leads to a decrease in auto-acceleration rate. If one compares auto-acceleration development rate for MMA and dimethyl acrylates (dMA), the following could be observed: the $W_{\max}/W_0$ ratio for MMA is 10–20 times higher than for dMA, and $\mathrm{d}W/\mathrm{d}C$ at the section with maximum rate of auto-acceleration development exceeds the same parameter for dMA from 100 to 200 times, while the $\mathrm{d}W/\mathrm{d}C$ value proper increases sharply as the conversion degree grows (for dMA, $\mathrm{d}W/\mathrm{d}C$ is virtually steady within the entire auto-acceleration range $0 < C < C_{\max}$).

The specific mechanism of diffusion mobility hindrance during TFRP is manifested in specific kinetic regularities related to correlation of effective reactivity

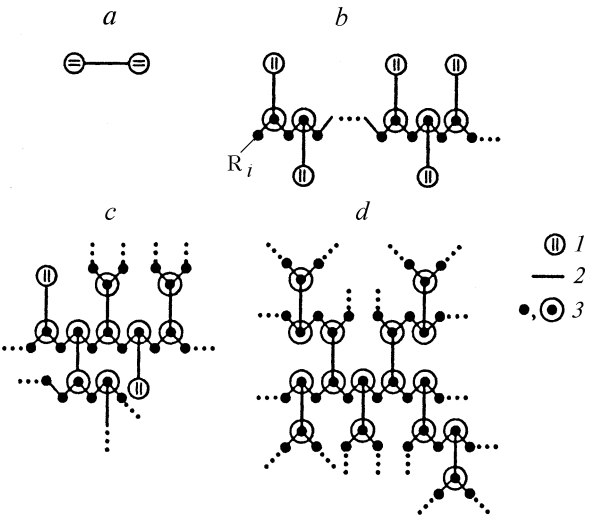

Fig. 2.4 Successive stages of TFRP for oligomers having two double bonds in their molecules: (***a***) initial state; (***b***) primary (nonbranched) polymer chain with "pendent" double bonds; (***c***) fragment of network with uncompleted structure (conversion < 1); (***d***) fragment of completed network (conversion ≈ 1); *1*, vinyl groups; *2*, oligomer blocks; *3*, secondary or tertiary carbon atoms with substituents H or R; R_I, initiator radical

of initial molecules with their physical (conformation) properties (molecule length, size of rotation barrier of constituent atomic groups). These regularities have been followed for large number of oligo(acrylates) of the following structure:

where the R_1 substituent refers to dicarboxylic acids, R_2 refers to glycols, and $n = 1$, 2 [1 (p. 165); 3 (p. 126); 39]. The oligomer synthesis method allowed varying the length and chemical composition of the oligomer block in a very wide range, with the end group type being the same.

At that, it is possible to separately vary a certain parameter (e.g., oligomer "length"), leaving all other parameters unchanged (nature of reactive groups; nature of groups determining internal rotation barriers and, in the final end, flexibility). Or, in contrast, it is possible to vary only sizes of internal rotation barriers while keeping all other parameters unchanged.

Results of studying the polymerization of oligo(acrylates) of different series, in which the length and chemical composition of the oligomer block changed in regular fashion, are listed in Tables 2.4 and 2.5; typical kinetic curves of polymerization with coordinates "reduced rate $W/[\mathrm{M}]$[1] – conversion C" are presented in Fig. 2.5. Effective reactive capacity of oligomers at constant temperature was characterized by parameters W, $W_{\max}$, $C_{\max}$, and $C_{\lim}$, where W = current polymerization rate in the range $W_0 < W << W_{\max}$, $C_{\max}$ = conversion corresponding to the maximum polymerization rate $W_{\max}$, and $C_{\lim}$ = maximum achievable conversion. In each homologous series of oligo(acrylates) with identical structure of oligomer block, the length of the latter varied (Table 2.4); in series I and II, with the length of oligomer block being almost invariable, the nature of diacid (family I) or glycolic (family II) and, hence, oligomer block flexibility, varied (Table 2.5). The internal rotation barriers of atomic groups of oligomer block decrease in series I in the following order:

$$-\mathrm{OOCC_6H_4COO}- > -\mathrm{OOC(CH_2)_4COO}- > -\mathrm{OOC(CH_2)_8COO}- > -\mathrm{OC(CH_2)_4S(CH_2)_4COO}-;$$

in family II:

$$-\mathrm{O(CH_2)_2O}- > -\mathrm{O(CH_2)_4O}- > -\mathrm{O(CH_2)_2O(CH_2)_2O}- > -\mathrm{O(CH_2)_6O}- > > -\mathrm{O(CH_2)_2O(CH_2)_2O(CH_2)_2O}-.$$

It was found that for identical reaction centers, i.e., end methacrylic groups, the effective reactive capacity of oligomers increases as the length and flexibility of oligomer blocks increase. Also, dependence of the effective reactive capacity on indicated physical (conformation) properties of initial molecules of oligo(acrylates) grows drastically as conversion degree increases; the most sensitive parameters are $W_{\max}$, $C_{\max}$, and, especially, $C_{\lim}$. For example, curves *1* and *2*, and *4* and *5* (see

[1] This relationship is convenient for determining main kinetic regularities of TFRP because $W/[\mathrm{M}] = K_{\mathrm{pr}}\sqrt{W_i/K_{\mathrm{ter}}}$ is an effective constant of polymerization rate at fixed temperature and initiation rate.

Table 2.4 Homologous series of oligo(acrylates)

Series of (meth)acrylates	General formula	Individual oligo(acrylates)						
		$n = 1$	$n = 2$	$n = 3$	$n = 4$	$n = 5$	$n = 6$	$n = 10$
Alkane diols	$\mathbf{M}(CH_2)_n\mathbf{M}$	–	dMAEG	dMAPDO	dMABDO	–	dMAHDO	dMADDO
(Diethylene glycol) phthalates	$\mathbf{M}(\mathbf{DP})_n\mathbf{DM}$	MDP-1	MDP-2	MDP-3	MDP-4	MDP-5	–	–
(Tetramethylene glycol) phthalates	$\mathbf{M}(\mathbf{BP})_n\mathbf{BM}$	MBP-1	MBP-2	MBP-3	–	–	–	–
		Increase of W, W_{max}, C_{max} and C_{lim} →						

Notation conventions for Tables 2.1, 2.4, and 2.5 only. Acidic residues: **M**, methacrylic; **P**, *ortho*-phthalic; alcoholic residues: **D**, diethylene glycol; **B**, tetramethylene glycol

Table 2.5 Series with various di[acids] and glycols

Series	Notation and repeated unit structure (in brackets) of series member				
I	MDP-1	MDA	MDS	MDU	–
	(MDPDM)	**(MDADM)**	**(MDSDM)**	**(MDUDM)**	–
	MEP	MBP-1	MDP-1	MHP	dMAtEGPh
II	**(MEPEM)**	**(MBPBM)**	**(MDPDM)**	**(MHPHM)**	**(MTPTM)**
Increase of W, W_{max}, C_{max} and C_{lim} →					

Notation conventions for Tables 2.1, 2.4, and 2.5 only. Acid residues: **M**, methacrylic; **P**, *ortho*-phthalic; **A**, adipinic; **S**, sebacic; **U**, 5,5'-thiodivaleric acid; alcohol residues: **B**, tetramethylene glycol; **H**, hexamethylene glycol; **D**, diethylene glycol; **T**, triethylene glycol; **E**, ethylene glycol.

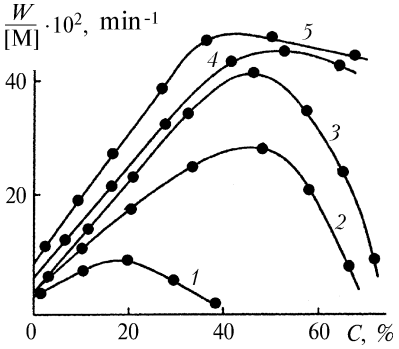

Fig. 2.5 Kinetics of polymerization of tested dMA series with different length (*1* and *2*, *4* and *5*) and size of internal rotation barriers of molecules with comparable lengths (*2* and *3*) TFRP substrates: $M-(CH_2)_n-M$, $n=4$ (dMABDO; curve *1*), $n=10$ (dMADDO; curve *2*); $M(CH_2)_2O(CH_2)_2O(CH_2)_2M$ (dMAtEG; curve *3*); $M[(CH_2)_2O(CH_2)_2O(O)C-Z-C(O)O]_n(CH_2)_2O(CH_2)_2M$, $n=1$ (MDP-1; curve *4*), $n=2$ (MDP-2; curve *5*). *M*, atomic group $CH_2=C(CH_3)C(O)O$; *Z*, aromatic fragment of *ortho*-phthalate. $T=70°C$; initiator, benzoyl peroxide (1% w.)

Fig. 2.5) refer to the analogous dMA (i.e., dMA having the same set of rotation barriers) with consistently increasing length of oligomer block. The reactive capacity enhances dramatically in the same sequence, especially at final stages of conversion, therefore, the limiting conversion for dMA with the shortest oligomer block $C_{lim} \to 40\%$ (curve *1*), and with sufficient chain length (curves *4* and *5*), auto-deceleration at the late stages virtually disappears and $C_{lim} \to 100\%$. Curves *3* and *4* (Fig. 2.5) refer to dMA with close lengths of oligomer blocks, but they are different in terms of sets of internal rotation barriers. In decandyol dimethacrylate (dMADDO, curve *2*) only two ester groups are hindered relatively weakly. In tri(ethylene glycol) dimethyl acrylate (tEGdMA, curve *3*), weakly hindered rotations of ether bonds are added to ester bonds, and, in the final end, enhancement of effective reactive capacity takes place as a result of transition from dMADDO to tEGdMA.

Parameters associated with the nature of oligomers proper, namely, length of the chain joining end methacrylate groups (oligomer block) and barriers of internal

rotation of atomic groups of the oligomer block, control the mobility of interjunction chains of the macromolecular network that is formed during TFRP. It is only oligomer blocks that become one of three interjunction chains of trifunctional junctions of the polymer network (see Fig. 2.4) after both methacrylate groups of dimethylacrylate react. Because two other interjunction carbon chains $-CH_2-$ are maximally short and rigid, it is just the third chain that provides junction relaxation which controls the mobility of elements of structured reaction medium: both the polymer network with pendent double bonds and diffusive mobility of molecules of nonreacted oligomers. As a result, the effective reactive ability of oligomers in TFRP in structured medium (at auto-acceleration and auto-deceleration stages) becomes enhanced as the probability of conformational transitions in the oligomer block of the polymer network increases.

The abnormal kinetic effect of ultrarapid TFRP under the conditions of photochemical initiation should be also interpreted within the framework of diffusion kinetics. In the case of high rates of photochemical initiation, initiating radicals $R_I^\bullet$ become main partners in the reaction of quadratic termination of chain $\sim R^\bullet + R_I^\bullet \rightarrow$ termination, where $R_I^\bullet$ is a radical small in size and, hence, highly mobile in a structured medium, while $\sim R^\bullet$ is a polymeric low mobile radical that is a chain carrier. This fact changes the polymerization kinetics quite dramatically: no auto-acceleration at all, and the order in terms of initiation rate changes from 0.5 (normal value) to 0 (anomaly) [40, 41]. The ultrarapid and easily controlled mode under the conditions of photochemical initiation at normal temperature made TFRP irreplaceable for the purpose of creation of high-tech polymer materials for microelectronics, fiberoptics, and data recording and storage devices [41–44].

Mathematical models of the TFRP process (auto-acceleration and auto-deceleration stages) are discussed in Sect. 2.5.

2.2 Inhibited Polymerization

The kinetics and mechanism of polymerization process inhibition, developing under specific conditions of TFRP were studied using inhibited oligo(acrylates) polymerization as an example. These studies are significant not only for understanding the inhibited TFRP mechanism, but also from the technological standpoint. Results of these studies of inhibited oligo(acrylates) polymerization are summarized in publications within the framework of homogeneous approach [1] (p. 194) and with peculiarities of the microheterogeneous TFRP mechanism taken into account [3] (p. 133).

Inhibited polymerization of oligo(acrylates) is of microheterogeneous character. Figure 2.6 shows kinetic dependencies reflecting influence of the quite effective inhibitor (X), benzoquinone (BQ), with $k_X/k_{pr} = 5.5$ at 44°C [45], where k_X and k_{pr} are reaction rate constants $\sim M^\bullet + X \xrightarrow{k_x}$ and $\sim M^\bullet + M \xrightarrow{k_{pr}}$, respectively. Because of such differences in rate constants, the inhibitor is mainly consumed at the early TFRP stage. Concentration X was varied, and for each [X] such concentration of

the initiator was selected that the reactive capacity at the initial TFRP stages is the same (curves *1–3* at $C < 20\%$). Dramatic difference in reactive ability with growing C cannot be explained without taking into account the microheterogeneous pattern of TFRP. Indeed, microheterogenization in the presence of X proceeds in such a way that the higher is the X concentration, the higher is the number of concurrently working self-contained micro-reactors (N_{lim}) in the reaction system [3, 46]:

$$N_{\text{lim}} = \frac{(k_{\text{X}}[\text{X}])^2}{(f-1)k_{\text{pr}}^2[\text{M}]_{\text{o}}} \tag{2.2}$$

where f = oligomer functionality and $[\text{M}]_0$ = initial concentration of oligomer.

Curves *1–3* in Fig. 2.6 are located correspondingly: the higher is [X], the higher is the effective reactive capacity.

The influence of microheterogeneity during inhibited oligo(acrylates) polymerization is demonstrated by comparison of kinetic behavior of one and the same inhibitor in two chemically identical systems that differ only in type of their structure formed sin the course of polymerization. Such comparison was conducted by the example of benzoquinone for chemically identical MMA and dMAtEG polymerizing in accordance with linear and tridimensional mechanisms, respectively. Kinetic parameters of inhibited polymerization are listed in Table 2.6: initial reduced rates $W/[\text{M}]_0$, fractions of induction period $\tau_{1/2}$, during which half of initially introduced inhibitor is consumed, i.e., $[\text{X}]_\tau/[\text{X}]_0 = 1/2$, which is indicated by twofold increase of polymerization rate as compared to the initial rate; the relationship of constant of radical-chain carrier and inhibitor reaction rate to that of radical-chain carrier and monomer reaction rate k_X/k_{pr} and, finally, stoichiometric coefficient of inhibitor μ.

By comparing k_X/k_{pr} and μ for MMA and tEGdMA, it is easy to see that benzoquinone has changed its properties as an inhibitor quite significantly during conversion to tEGdMA: the k_X/k_{pr} relationship increases approximately 1.5 times, while μ, in contrast, decreases almost 4 fold. As from the chemical standpoint both systems, MMA and tEGdMA, are absolutely identical, the observed effect could be explained by structure formation during inhibited polymerization of tEGdMA.

Oligo(acrylates) synthesis and storage, as well as oligo(acrylates) processing via polymerization into finished goods, are possible only through the application of

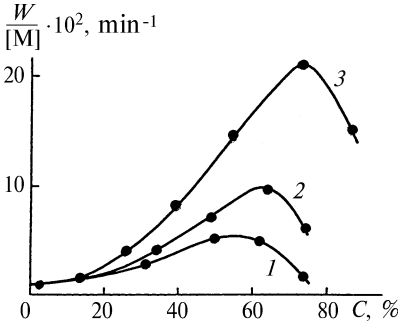

Fig. 2.6 Polymerization of dMA-tEGPh with fixed molar relationship: initiator (DCPD)/inhibitor (BQ) = 1:1. Initiator and inhibitor concentration, % (by weight): *1*, 2; *2*, 4; *3*, 6. $T = 35°\text{C}$

Table 2.6 Parameters of MMA and tEGdMA polymerization inhibited with BQ

Concentrations of initiator and inhibitor $\times 10^3$, mol/l		MMA				tEGdMA			
AIBN	BQ	$\frac{W}{[M]_0}\cdot 10^3$, $\min^{-1}$	$\tau_{1/2}$, min	K_X/k_{pr}	μ	$\frac{W}{[M]_0}\cdot 10^3$, $\min^{-1}$	$\tau_{1/2}$, min	K_X/k_{pr}	μ
10	2	0.27	310	5.0	2.0	0.41	128	11	0.49
	5	0.14	1030	4.1	2.3	0.16	460	10	0.45
20	2	0.59	149	5.5	1.8	0.74	68	8.5	0.51
	–	0.43	146	6.0	2.0	–	–	–	–
	5	0.26	345	5.4	1.7	0.42	184	6.8	0.50
	–	0.23	400	5.1	2.0	–	–	–	–
	10	0.18	613	5.6	2.1	0.24	400	7.0	0.40
40	2	0.94	92,5	5.6	2.2	1.48	41	8.3	0.57
	–	0.92	90	6.3	2.0	–	–	–	–
	5	0.43	188	6.6	1.7	0.65	115	8.3	0.52
	–	0.46	184	6.0	1.7	–	–	–	–
	Mean value			≈5.5	≈1.9	–	–	≈8.6	≈0.5

Note. Temperature 60°C, initiator, 2,2′-azobis (2-methylpropionitrile) (AIBN).μ, stoichiometric coefficient of inhibitor

adequate inhibitors that prevent spontaneous polymerization of oligomers. Generalization of data on inhibited oligo(acrylates) polymerization [1, 3] leads to a conclusion that none of the known inhibitors or their combinations have features of the so-called ideally overlapping inhibitors. This term means an inhibitor so highly effective that its presence in a polymerization system decreases the kinetic chain length to the limiting low value (about 1), so that the polymerization process becomes almost completely suppressed for some period of time τ (induction period), during which the inhibitor is fully consumed. After lapse of time τ, polymerization proceeds as a noninhibited process, i.e., the ideal inhibitor action takes place only during period τ without leaving any "traces" in the course of subsequent polymerization, with the exception of influence on stationary concentration of polymer grains. Value τ in this case is directly proportional to inhibitor concentration and reversely proportional to the "overlapping" initiator concentration. If the latter parameter value is less compared to the inhibitor concentration (molar concentrations are compared here), value τ becomes infinity (i.e., concentration is insufficient for overlapping). The action of inhibitors (that are less effective than the ideal one) differs in the fact that the kinetic chain length during inhibition period τ is considerably greater than 1; therefore, a part of the polymerization process (or even the entire polymerization process) proceeds in the presence of inhibitor. The more such nonideal inhibitors complicate the vitrification mode for oligo(acrylates) and impair properties of polymerizates, the more different they are from the ideal ones. The inhibitor efficacy, in other words, the inhibition rate constant k_X, represents a measure for the approximation to the properties of ideal inhibitors. Information on values of

k_X of inhibitors of different classes is given in a monograph [45] and a reference book [47].

The inhibitor ideality degree was suggested to be quantified by an "ideality parameter" θ [3] (for ideal inhibitor: $\theta = 1$). Nonideality of behavior ($\theta < 1$) in the case of low-effective inhibitors (the so-called retarding agents) characterized by $k_X \leq k_{pr}$, where k_X and k_{pr} are reaction rate constants for the reaction of propagation radical with molecule X and oligo(acrylates), respectively, has rather trivial explanation: it follows from $k_X \leq k_{pr}$ that the inhibitor consumption rate during polymerization conversion does not exceed oligo(acrylates) consumption rate, hence, the inhibitor is present in the reaction system right to the very end of polymerization. In this case quadratic termination of chains $\sim\mathbf{M}^{\bullet} + \sim\mathbf{M}^{\bullet}$ limited by diffusion due to large size of $\sim\mathbf{M}^{\bullet}$ (macroradicals, a part of which is linked with the network) is replaced with linear termination $\sim\mathbf{M}^{\bullet} + \mathbf{X}$ with participation of small (highly mobile) molecules X, and the diffusion control over linear termination is expressed to a much lower extent. Therefore, at a certain inhibitor concentration (curve *2*, Fig. 2.7), the kinetics characteristic of TFRP (auto-acceleration – maximum – auto-deceleration) transforms in such a way that the auto-acceleration stage disappears completely, while the auto-deceleration stage is shifted to the region of very high conversions.

For effective inhibitors characterized by $k_X > k_{pr}$, quite significant deviation from ideality could be explained both by transformation of inhibitors X during the inhibition reaction into secondary products X′ possessing retarding agent properties and by specific features of TFRP proceeding according to the microheterogeneous mechanism. Theoretically, this may happen only in the case when microheterogeneous structures have enough time to be formed during induction period τ (i.e. before the introduced inhibitor is fully consumed).

Then, polymerization inhibited by the remaining inhibitor should proceed under specific conditions of complicatedly structured medium, i.e., in a medium consisting of grains or their nuclei surrounded with unreacted initial oligo(acrylates) and having transition zones that consist of peripheral layers of grains and fringe. Under these conditions, inhibitor molecules may turn out to be outside the intensive polymerization conversion zone (for instance, because of microredistribution), and the inhibitor, entering into this zone via diffusion from micro-reservoirs with quasi-constant concentration, would behave as a weaker one, but possessing more expressed prolonged action.

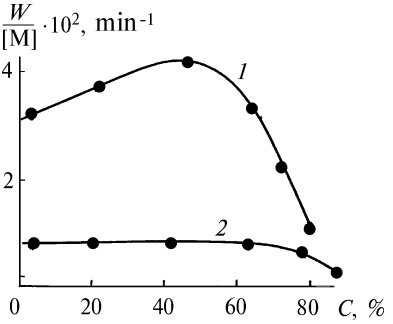

Fig. 2.7 Polymerization of tEGdMA in the presence of TNT inhibitor (2,4,6-trinitrotoluene) acting throughout the entire TFRP process: *1*, $[TNT] = 5 \times 10^{-3}$ mol/l; *2*, $[TNT] = 3 \times 10^{-2}$ mol/l. $T = 60°C$; initiator, AIBN, [AIBN] = 0.02 mol/l

In other words, the local active mass of inhibitor $[X]_{loc}$ might turn out to be much lower than its volume-averaged effective concentration [X], as a result of which the inhibiting effect proportional to the product of $k_X[X]_{loc}$ would be diminished, but the time of inhibitor action would be prolonged by feeding of $[X]_{loc}$ by [X]. It is obvious that starting from the moment when $[X]_{loc} << [X]$, the subsequent consumption of inhibitor would also take place in diffusion-limited feeding mode $[X] \rightarrow [X]_{loc}$; the inhibitor would behave as essentially nonideal ($\theta < 1$). Indeed, a reduction of inhibitor active mass caused by structure formation from level [X] to $[X]_{loc}$, on the one hand, would lead to polymerization rate growth during induction period that in practice is similar to reduction of τ, and, on the other hand, would result in diminution of polymerization rate after τ, as compared to noninhibited polymerization, which is equivalent to an increase in hardening time of three-dimensional structure formation.

Those inhibitors were trial tested for oligo(acrylates) polymerization, the effectiveness of which varied within a very wide range: from low-effective ones, such as 2,4,6-trinitrotoluene with $k_X/k_{pr} = 0.05$ and $k_X = 231/(\text{mol} \cdot \text{s})$ at 44°C [45], to the most highly effective ones, such as stable nitroxyl radicals with $k_X = 6 \cdot 10^5 1/(\text{mol} \cdot \text{s})$ at 60°C [45]. In all cases, $\theta < 1$ and a high value of k_X in relation to k_{pr} is only a necessary but not sufficient feature of the ideal inhibitor.

The issue of raising the efficiency of inhibitors (bringing their properties closer to those of the ideal inhibitor) is usually solved through the use of synergists [1, 3]. The application of styrene as a synergist for the inhibited oligo(acrylates) polymerization was suggested and theoretically substantiated [1, 48]. In this case, partial substitution of radical-chain carrier for another radical having higher reactive capacity in relation to a given inhibitor molecule takes place. The substitution is implemented by adding to the reaction system a certain substance, which is able to react easily with the radical-chain carrier, thus forming new free radical.

In the case of styrene added to oligo(acrylates) that contains benzoquinone, the methacrylic radical-chain carrier, after reacting with styrene, is transformed into styrene radical, which is incommensurably more reactive in relation to benzoquinone versus methacrylic radical [styrene radical $k_X/k_{pr} = 518$ and $k_X = 1 \times 10^5 1/(\text{mol} \cdot \text{s})$ at 50°C, and methacrylic radical $k_X/k_{pr} = 5.5$ and $k_X = 2.6 \cdot$

Table 2.7 Effect of styrene additives on benzoquinone (BQ) overlapping for tEGdMA polymerization

BQ concentration, % (by weight)	Styrene concentration, % (by weight)	τ, min	θ	BQ concentration, % (by weight)	Styrene concentration, % (by weight)	τ, min	θ
0	0	2	–	0.002	0.13	6	0.30
0.001	–	3.5	0.55	0.002	0.50	10	0.35
0.002	–	4.5	0.38	0.002	1.00	11	0.55
0.004	–	7.5	0.17		–	–	–
	–	–	–	0.004	0.13	8	0.20
0.001	0.50	8	0.55	0.004	0.50	13	0.30
0.001	1.00	8	0.63	0.004	1.00	24	0.39

Note. Temperature, 35°C; initiator, dicyclohexylperoxydicarbonate (DCPD), 1.4×10^{-2}mol/l.

$10^3 1/(\text{mol} \cdot \text{s})$ at 44°C when reacting with benzoquinone] [45]. As a result, the inhibitor efficiency (effective value of k_X) increases dramatically and, thus, styrene manifests its property as a synergist (Table 2.7).

This is one of the few cases of synergetic effect for which the mechanism has been clearly determined and a quantitative theory has been formulated, enabling one to calculate the effective rate constant k_X as a function of concentration of inhibitor and styrene [1, 48].

2.3 Polymerization in Solutions

Results obtained when studying TFRP in solvents provide valuable data on the polymerization process mechanism both at the very beginning of polymerization and in structured reaction medium. This section presents data related to those polymerization stages, when a microheterogeneous structure consisting of polymeric highly cross-linked grains separated by low cross-linked interlayers serves as a reaction medium.

Typical kinetic results illustrating the solvent effect were obtained by an example of tEGdMA oligomer polymerization in the presence of 0–60% (by volume) various solvents: three good ones (benzene, acetonitrile, DMFA) (Fig. 2.8) and a poor one (heptane) (Fig. 2.9) [5 (p. 109); 49].

It can be seen that the effect of good solvents (thermodynamic quality is meant) is manifested kinetically as an increase in polymerization rate at all conversions, and this increase progresses with growing degree of conversion C, and at the auto-deceleration stage it becomes total; the rate increases by orders of magnitude with concurrent shift of limiting conversion into the area of high C. Also, one of the three good solvents, namely, DMFA, exhibits qualitative changes of kinetics pattern at late stages: auto-deceleration at first is shifted to the area of higher C as solvent concentration grows and then it disappears completely (Fig. 2.8c, curve *5*). Limiting (quasi-complete) conversion associated with auto-deceleration also disappears, and polymerization proceeds until complete conversion ($C \approx 100\%$) with auto-acceleration. The poor solvent, i.e., heptane, shows the reverse kinetic effect (Fig. 2.9): as solvent concentration increases, the polymerization rate declines at all conversion stages, and this decline progresses as C increases, reaching very high values at the auto-deceleration stage, which, in the final step, is manifested as a shift of limiting degree of polymerization to the low-degree conversion area.

It would be well to relate kinetic effects of good solvents, first of all, to an increase in volumes of shell layers or reaction zones of polymer grains (see Fig. 1.8) from additional swelling and, as a consequence of this increase, to the growth of actual total reaction volume with corresponding increase of polymerization rate measured experimentally. Also, it is assumed that possible reduction in the concentration of nonreacted oligomer in the reaction zone (due to dilution) is not sufficient to compensate for this additional increase. Additional swelling of the shell layers may happen because of better affinity of solvent as compared to initial oligomer or higher thinning of macromolecular network in the shell layers

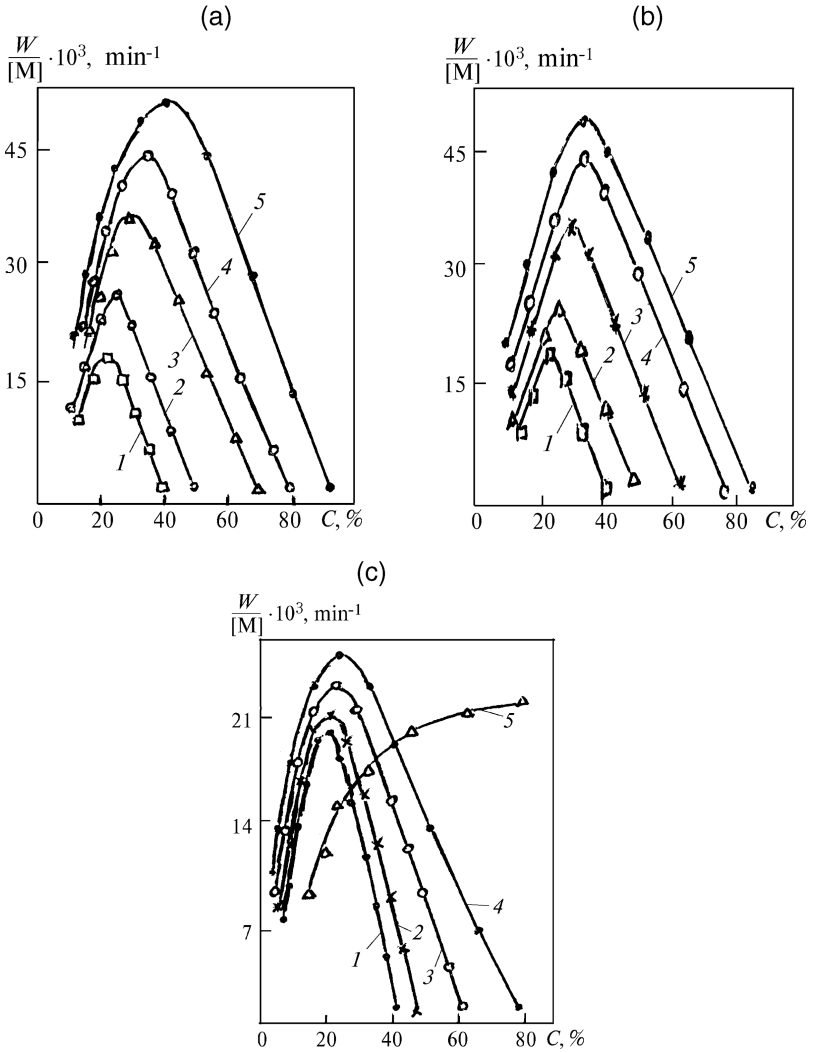

Fig. 2.8 Dependence of reduced rate of tEGdMA polymerization in solutions of acetonitrile (***a***), benzene (***b***), and DMFA (***c***) upon conversion tEGdMA concentration, % (by volume): *1*, 100; *2*, 80; *3*, 60.0; *4*, 50.0; *5*, 40.0. $T = 40°C$; $[DCPD] = 2.6 \times 10^{-3}$mol/l

resulting from dilution. The first assumption is not true because it is not confirmed by experimentally determined sequences on thermodynamic activity (affinity to tEGdMA polymer), in which the parent oligomer occupies a higher place than other solvents: oligomer > benzene ≈ DMFA > acetonitrile > heptane [50]. In addition, absolute values of maximum reduced polymerization rates $W/[M]$ attained in case of high-degree dilutions differ quite considerably for selected good solvents: from $W/[M] = (45–50) \times 10^{-3}$ min^{-1} for benzene and acetonitrile to $W/[M] = 25 \times 10^{-3}$ min^{-1} for DMFA; and this sequence of kinetic activity of

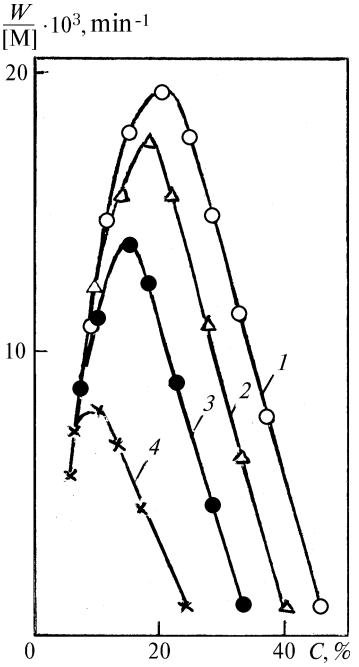

Fig. 2.9 Dependence of reduced rate of tEGdMA polymerization in solutions of heptane upon conversion. tEGdMA concentration, % (by volume): *1*, 100; *2*, 90.0; *3*, 80.0; *4*, 70.0. $T = 40°C$; $[DCPD] = 2.6 \times 10^{-3} mol/l$

solvents, i.e., benzene $\approx$ acetonitrile $>$ DMFA, does not match the thermodynamic activity sequence. Therefore, we have to believe that the reason for additional growth of volume of the near-surface layers in the presence of good solvents is an increased degree of thinning of their network structure.

One of the most probable mechanisms for thinner network at periphery of grains consists in the following. Radial flow of "initial oligomer + solvent" compound is generated by denser packing of network structure of grains, and this denser packing develops successively from grain center to periphery (microsyneresis) (see Sect. 1.3.1). As a result of polymerization, this flow is depleted of the first component, the oligomer, while concurrently enriched with the second component, i.e., the solvent. Specific dynamic concentration of oligomer in the radial flow appears only as a result of counter diffusion flow of nonreacted initial oligomer from the ambient. As initial solvent concentration and conversion degree grow, this dynamic concentration of oligomer may reach indefinitely small values in the shell layers located far enough from highly cross-linked cores of grains. Correspondingly, an indefinitely low cross-linked macromolecular structure will be formed in these layers, which would possess high ability to swell in good solvents. It is well known that such swollen shells [51] prevent aggregation processes by using a mechanism of the so-called polymeric stabilization of dispersion. Therefore, in the presence of good solvents, the probability of grains aggregation is decreased with corresponding diminution of reaction volume and, hence, the tendency for auto-deceleration of polymerization process is degraded at later stages, up to complete disappearance of the auto-deceleration stage. Special experiments showed [52] that introduction of

additives of polymer dispersion stabilizers of different types into a reaction system, such as colloxylin, polisoprene surfactants (see Sect. 1.2.2, Fig. 1.7), results in elimination of auto-deceleration, which may serve as an indirect confirmation of correctness in interpreting the effects of good solvents upon late stages of oligo(acrylates) polymerization. In the case of a poor solvent, i.e., heptane, it is likely that a reduction in the volume of the sparse shell layer of polymer grains takes place due to diminution of swelling degree (precipitation effect) with corresponding kinetic consequences.

A model system was used to evaluate thermodynamic qualities of a reaction medium with respect to cross-linked polymers tEGdMA. The role of polymer in this model system was played by poorly branched soluble products of tEGdMA polymerization (the so-called β-polymers), while the role of reaction medium was played by tEGdMA oligomer or solution of tEGdMA oligomer in benzene or other solvents. The thermodynamic quality of the medium was estimated by the temperature dependence of light-scattering intensity R during temperature scanning from 20° to 80°C [50]. The presented data indicate that, for the temperature range $20° - 80°$C, oligomer, DMFA, and benzene are good solvents for tEGdMA polymers, and, in contrast, heptane is a poor solvent. Acetonitrile, the thermodynamic affinity of which to oligo(acrylates) polymers is higher than that of heptane but significantly lower than that of benzene, DMFA, or tEGdMA oligomer, occupies an intermediate position.

Thus, the presented data verify that kinetic specifics of three-dimensional free-radical polymerization in a structured reaction medium are determined by conformation properties of parent unsaturated oligomers (such as molecule length and internal rotation barriers) and by the action of reaction medium (solvents, surfactants, inhibitor dopes) that influence the aggregation processes of polymer chains (inhibitors with $k_X > k_{pr}$) and the type of chain termination (inhibitors with $k_X < k_{pr}$). The effective reactive capacity of unsaturated oligomers at the initial stage of three-dimensional free-radical polymerization (with initial rate W_0) with conversion $C \to 0$ (unstructured reaction medium) is determined by other factors, namely, by oligomer viscosity and their capability to produce regular kinetically active associates.

2.4 Polymerization in Films Under the Conditions of Oxygen Diffusion

TFRP processes with participation of air oxygen represent a chemical basis for film formation from unsaturated oligomers that are one of the most popular substances among modern industrial-scale film-forming substances [53]. TFRP in liquid oligomers films applied onto substrates and in an oxygen-containing atmosphere is characterized by kinetic specifics that differ significantly from block or solution polymerization [2]. These specifics, as it was found through systematic studies

[2] Results of studying kinetics and mechanism of oxidative polymerization of unsaturated compounds in block and solution are described in monographs [2, 4] and review [58].

[2, 4], are preconditioned by the fact that polymerization (including TFRP) is represented by copolymerization of oligomers with oxygen (oxidative polymerization) and homo-polymerization. The relationship of these conjugated reactions changes in films layer by layer together with changing conversion degree depending on layer-by-layer variation in the concentration of oxygen diffusing into the film. Also, kinetic specifics of TFRP for compounds of vinyl and allyl types [3] in films should be analyzed taking into account the different reactivity of these compounds in reactions of radical addition and radical substitution.

2.4.1 Vinyl Compounds

2.4.1.1 Kinetic Specifics of Oxidative Polymerization of Vinyl-Type Compounds in Films Under the Conditions of Oxygen Diffusion

These specifics have been studied by an example of polymerization of the following oligo(acrylates)s: dimethyl acrylate of (bis-ethylene glycol)adipate (dMA-EGA), tetra(meth)acrylate of (bis-trimethylolpropane)adipate (teMA-tPA), and hexamethacrylate of (bis-pentaerythrite)adipate (hMA-PeA) [4 (p. 151); 54]. Oligomers were polymerized together with a redox system introduced in concentration of 2.28×10^{-2}mol/l (0.55% by weight) of di(1-hydroxycyclohexyl) peroxide (DHHP) and 1.07×10^{-2}mol/l (0.05% by weight) of cobalt naphthenate (calculated per metal cobalt) at initiation rates W_i 8.2×10^{-6}, 2.0×10^{-5}, and 6.6×10^{-5}mol/(l·s), respectively, at 65°, 80°, and 100°C.

Oxygen absorption was measured by the circulation volumometry method using a specially designed instrument [55]. Kinetic curves of O_2 absorption reflect exactly the kinetics of oxidative polymerization (copolymerization of oligomer with oxygen in reactions $\sim M^{\bullet} + O_2 \xrightarrow{k_1} \sim MO_2^{\bullet}(1)$ and $\sim MO_2^{\bullet} + M \xrightarrow{k_1} \sim MOOM^{\bullet}(2)$, because in identical conditions the oxidation rate of saturated organic compounds that simulate the structures of oligomer blocks dMA-EGA, teMA-tPA, and hMA-PeA is 15–20 times lower than that of these oligo(acrylates)s. This result means that the hydrogen abstraction reaction $\sim MO_2^{\bullet} + MH \xrightarrow{k_2'} \sim MOOH + M^{\bullet}(2')$ can be neglected up to conversion degrees C = 90–95% in terms of double bonds.

The influence of structure for oxidative polymerization is manifested in the fact that oxygen absorption rate W_{O_2} grows as molecular functionality f increases, while limiting conversions C_{O_2} diminish (Figs. 2.10 and 2.11).

Autocatalytic character of oxidative polymerization most likely stems from changes in medium viscosity as a result of polymer product accumulation.

During development of auto-acceleration, soluble polymers [56] with the polymer chain length of ≈10 oligomer units, the translational diffusion coefficient of

[3] Double bonds of vinyl-type compounds are highly reactive in radical addition reactions. Double bonds in the allyl-type compounds are characterized by low activity in radical addition reactions, while allyl compounds proper are highly reactive in radical substitution reactions.

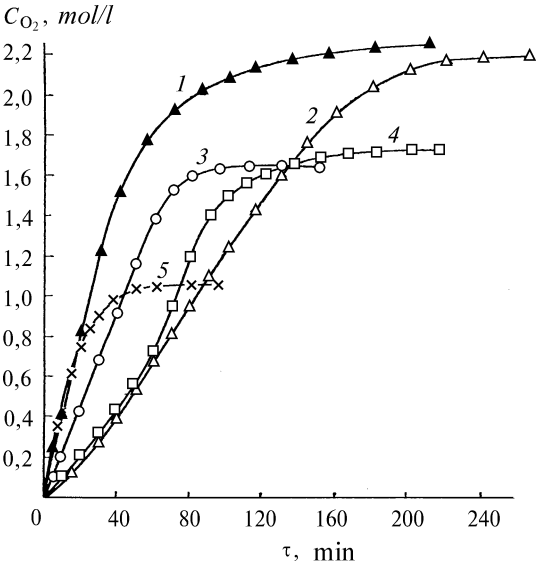

Fig. 2.10 Kinetic curves of oxygen absorption during oligo(acrylates) polymerization in films with thickness of 35 μm at $P_{O_2} = 21$ kPa: *1* and *2*, dMA-EGA, 100° and 80°C; *3* and *4*, teMA-tPA, 80° and 65°C; *5*, hMA-PeA, 65°C

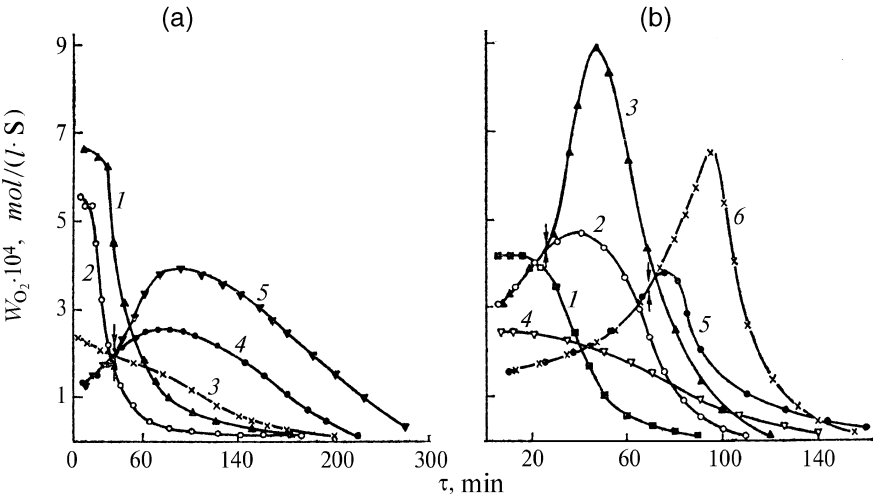

Fig. 2.11 Dependence of W_{O_2} on duration of dMA-EGA (***a***) and teMA-tPA (***b***) polymerization in films with different thickness at $P_{O_2} = 21$ kPa: (***a***) *1* and *2*, 100°C, 35 and 80 μm; *3*, *4*, and *5*, 80°C, 80, 35, and 15 μm; (***b***) *1*, *2*, and *3*, 80°C, 80, 35, and 15 μm; *4*, *5*, and *6*, 65°C, 80, 35, and 15 μm. *Arrows* indicate points corresponding to conversion $C_{lim} \approx 1 - 3\%$

which does not exceed 10^{-7}cm^2/s [10 (p. 178)], serve as peroxide radical carriers. Under these conditions, quadratic termination should be controlled by diffusion, and auto-acceleration of gel-effect type becomes probable.

However, specifics of oxidative polymerization are not exhausted by trivial development of autocatalysis according to gel-effect mechanism. It was established that process kinetics depends heavily upon film thickness (Figs. 2.11 and 2.12) and

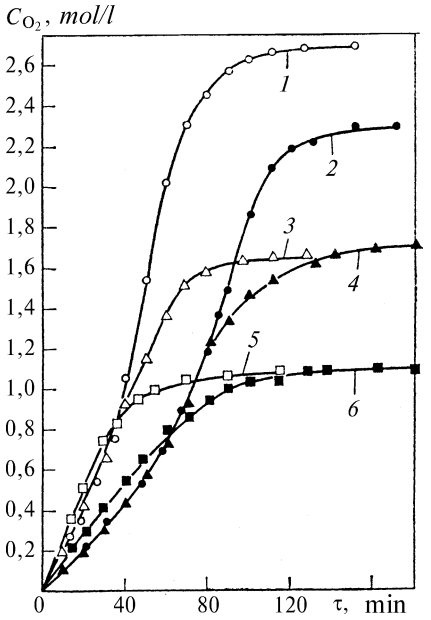

Fig. 2.12 Kinetic curves of oxygen absorption during teMA-tPA polymerization in films with different thickness when $P_{O_2} = 21$ kPa: 1, 3, 5, 80°C, 15, 35, and 80 μm; 2, 4, 6, 65°C, 15, 35, and 80 μm

partial pressure of oxygen in the gas phase (Fig. 2.13), namely: as a rule, autocatalysis degree and limiting conversions are inversely dependent upon film thickness, and they grow as partial oxygen pressure P_{O_2} increases. In some cases, coincident sections of kinetic curves are observed for films of different thickness (Figs. 2.11 and 2.12) and different values of P_{O_2} (Fig. 2.13), and the length of these sections grows with increasing P_{O_2}. The reaction in films with the thickness of 80μm turns out to be sensitive to P_{O_2} and film thickness practically from the beginning of measurements (Figs. 2.12 and 2.13).

It is impossible to interpret the presented experimental data without using a *layered model of oxidative polymerization in films* [54]. The model is based on the following fundamental notions. Before the beginning of polymerization, oxygen $[O_2]_0$ concentration is the same in all film layers and is determined by oxygen solubility γ in the oligomer and partial pressure of oxygen P_{O_2} above the film $[O_2]_0 = \gamma P_{O_2}$. With the beginning of polymerization, the diffusion flux of oxygen from the gas phase into the film is generated as a result of oxygen consumption, and positive gradient $[O_2]$ is observed throughout the film thickness from substrate to surface. Changes of $[O_2]$ in the i-th film layer are determined by difference of oxygen consumption rate $W^i_{O_2}$ and oxygen diffusion W^i_D into the i-th layer. Value W^i_D is derived from the following expression [57]:

$$W^i_D = D^i_{o_2}([O_2]_o - [O_2]_i)/l_i^2 \tag{2.3}$$

The value of W^i_D is inversely proportional to squared distance from film surface to the i-th layer and is determined by gradient $[O_2]$ and diffusion coefficient $D^i_{O_2}$,

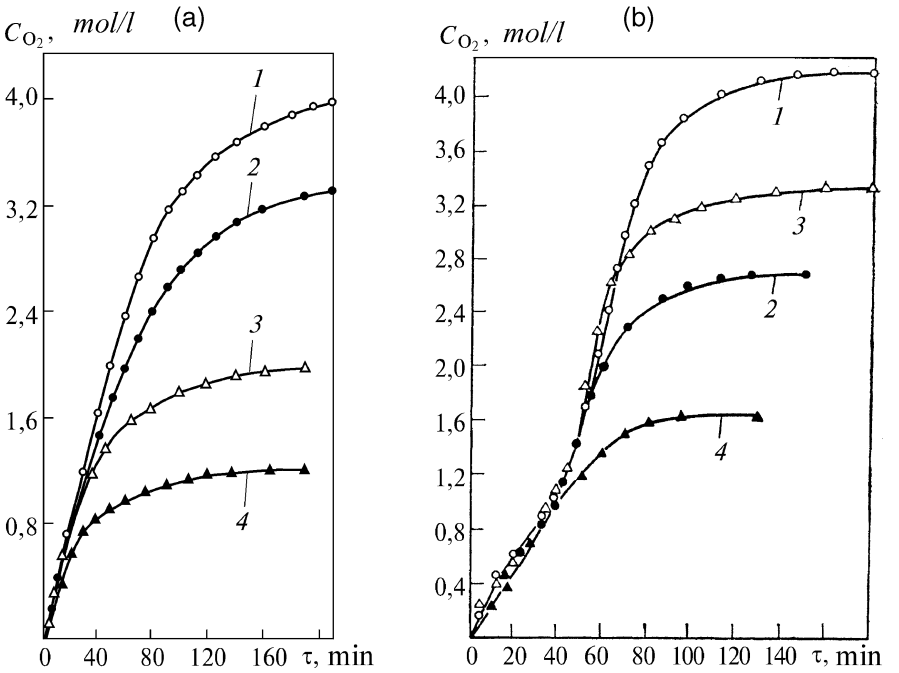

Fig. 2.13 Kinetic curves of oxygen absorption during dMA-EGA polymerization at 100°C(***a***) and teMA-tPA polymerization at 80°C(***b***) with different values of P_{O_2}: (***a***)*1*,*3*,35 μm, 100 and 21 kPa; *2*,*4*,80μm, 100 and 21 kPa; (***b***)*1*,*2*,15 μm, 100 and 21 kPa; *3*,*4*,35 μm, 100 and 21 kPa

which, in the discussed case, is a function of reaction medium viscosity η, and $D^i_{\mathbf{O}_2} = f(1/\eta)$. The value of $W^i_{\mathbf{O}_2}$ is found from the following equation:

$$W^i_{O_2} = W_I \cdot \nu \tag{2.4}$$

where W_I = initiation rate, and ν = average length of kinetic chains of processes with oxygen participation.

Starting from certain conversion C (which depends upon film thickness, partial pressure of oxygen above the film, initiation rate, and oligomer oxidability in the film layer, which is farthest from the surface), a situation would inevitably occur when oxidative polymerization rate $W_{\mathbf{O}_2}$ is limited by the rate of oxygen diffusion into film $W_{\boldsymbol{D}}$. The inevitability stems from the fact that $W_{\mathbf{O}_2}$ grows continuously (gel effect) as a result of medium viscosity growth, which results from accumulation of polymer products, while the value of $W_{\boldsymbol{D}}$ goes down.

As the polymer accumulation rate in the first layer (adjacent to the substrate) is always higher than that in any of the further layers located above the first one due to lower stationary concentration of inhibitor (i.e. oxygen), the viscosity of the first layer changes the fastest, resulting in a corresponding decrease of the constant of chain termination rate and, therefore, in growth of $W_{\mathbf{O}_2}$. However, the growth of $W_{\mathbf{O}_2}$ is constrained by the limit of $W_{\boldsymbol{D}}$. This limiting value $W^{(1)}_{\mathbf{O}_2\,\mathrm{lim}} = W^{(1)}_D$ (where

index 1 denotes layer number) is the higher, the closer is the layer to the surface (the value of $W_D^{(i)}$ is inversely proportional to l_i^2).

Then, as the oxidative polymerization process develops further (with corresponding growth of medium viscosity), the oxygen absorption rate in the second layer reaches the limiting value $W_{O_2\,\mathrm{lim}}^{(2)} = W_D^{(2)}$, and then the similar situation develops in the third layer: $W_{O_2\,\mathrm{lim}}^{(3)} = W_D^{(3)}$ and so forth. In this process, $W_{O_2\,\mathrm{lim}}^{(1)} < W_{O_2\,\mathrm{lim}}^{(2)} < W_{O_2\,\mathrm{lim}}^{(3)} \ldots$, because $w_D^{(1)} < W_D^{(2)} < W_D^{(3)} \ldots$ due to $l_1 > l_2 > l_3 \ldots$, i.e., the polymerization front, satisfying the requirement $W_{\boldsymbol{D}} = W_{\mathbf{O}_2\,\mathrm{lim}}$, moves forward layer by layer from the substrate to the film surface. Each layer passes successively through one and the same set of corresponding viscosity states, but with different and growing degrees of conversion. Starting from the moment when condition $W_{O_2\,\mathrm{lim}} = W_D$ is satisfied in the lowest film layer with thickness l, integral rate of oxidative polymerization $\overline{W}_{\mathbf{O}_2}$[4] for any film with thickness $l' < l$ turns out to be higher than that for a film with thickness l. Increasing the partial pressure of oxygen should be equivalent (in terms of its influence on oxidative polymerization development) to film thickness reduction because $W_{\boldsymbol{D}} \sim P_{\mathbf{O}_2}$. The value of auto-acceleration for the oxidative polymerization decreases as the polymerization front propagates with $W_{\boldsymbol{D}} = W_{\mathbf{O}_2}\,\mathrm{lim}$, and at a certain degree of conversion, auto-deceleration begins, which satisfies condition $\overline{W}_D < \overline{W}_{O_2}$. Thus, the autocatalysis degree of the oxidative polymerization according to the layered model (all other factors being equal) should depend upon film thickness and partial pressure of oxygen above the film.

Indeed, in thinner films and in case of higher partial pressures of oxygen, the autocatalysis rates and degrees are higher (see Figs. 2.11, 2.12, and 2.13). Coincident sections of curves $W_{\mathbf{O}_2} = f(\tau)$ (Fig. 2.11) for films that differ in thickness correspond to the reaction medium state, when oxygen consumption rate (even in the deepest layers of thicker film) has not yet reached $W_{\mathbf{O}_2\,\mathrm{lim}}$ and, therefore, does not depend upon thickness value [kinetic mode of oxidative oligo(acrylates) polymerization]. In this mode, the stationary concentration of oxygen in all film layers is virtually equal to oxygen solubility in the substrate. Splitting points of coincident sections of curves correspond to the transition of reaction in lower film layers with thickness of 35 μm into the diffusion mode. Location of splitting points and maximums on curves $W_{\mathbf{O}_2} = f(\tau)$ depend upon oligo(acrylates) structure and film-forming conditions.

Viscosity variation rate $d\eta/d\tau$ increases as molecular functionality enhances in terms of double bonds and temperature. Therefore, the area of oxidative polymerization development in the kinetic mode in the case of dMA-EGA is larger than for teMA-tPA. Temperature drop exerts a similar influence upon each of the oligo(acrylates)s. For the same reason, the auto-acceleration period in films with thickness 80 μm ends very quickly, and thus researchers fail to register this period in experiments (Fig. 2.11). Dropping branches of curves $W_{\mathbf{O}_2} = f(\tau)$ are determined by a trivial reason, namely, by dramatic diminution of $D_{\mathbf{O}_2}$ at deep conversions caused by film solidification.

[4] In experiments, it is just the integral process rate (averaged throughout the film volume) that is actually measured.

The afore-described interpretation of experimental data is verified by the character of dependency of kinetics of oligo(acrylates) interaction with oxygen upon partial pressure of oxygen P_{O_2} (see Fig. 2.13). Rates on coincident sections of curves do not change with increasing P_{O_2} (kinetic mode of oxidative polymerization); at the same time, the length of these sections increases considerably due to the growth of W_D, as a result of which W_{O_2} lim also increases. Increase of W_D with growing P_{O_2} also determines an increase of $C_{O_2\,lim}$ and maximum rates of oxygen consumption at late stages of reaction, when W_{O_2} is determined by the value of W_D. For the same reason, smoothing of differences is observed in kinetics of oligo(acrylates) interactions with oxygen between thin and thick films. Increased film thickness, as well as increased medium viscosity (up to gel consistency), lowers the oxygen diffusion rates to such values that are less or comparable with oxygen consumption rates, thus switching over the oxidative polymerization reaction into diffusion mode. As a rule, switching-over between the modes of oxidative polymerization occurs in the gel-formation area with the content of cross-linked polymer being within 1–3% (see Fig. 2.11).

Thus, the layered model adequately reflects the main kinetic specifics of oxidative polymerization of oligo(acrylates) in films under the conditions of oxygen diffusion.

2.4.1.2 Kinetic Features of TFRP of Vinyl-Type Compounds in Films Under the Conditions of Oxygen Diffusion

Kinetic features of TFRP inhibited by oxygen diffusing into the film were studied taking the polymerization of oligo(acrylates) with different functionality as an example [2, 4]. Oxygen inhibits methacrylate polymerization [including oligo (acrylates)] due to highly effective transfer of chain to oxygen $\sim M^{\bullet} + O_2 \xrightarrow{k_1} \sim MO_2^{\bullet}(1)(k1 = 1 \times 10^7 1 \cdot mol^{-1} \cdot s^{-1})$ at 50°C for MMA [47]) and slow regeneration of chain by peroxide radicals $\sim MO_2^{\bullet} + M \xrightarrow{k_2} \sim MOOM^{\bullet}$ (2) [4]. The rate of reaction (2) is lower than the chain propagation rate $\sim M^{\bullet} + M \xrightarrow{k_3} \sim MM^{\bullet}(3)$ ($k_3/k_2 \approx 200$, MMA at 50°C) [2, 4, 58]. The ratio of rates of competing reactions of chain transfer to oxygen and chain propagation $\sim M^{\bullet} + M \xrightarrow{k_3} \sim MM^{\bullet}$ (3) for oligo(acrylates) polymerization depending on $[O_2]$ is given in Table 2.8.

Table 2.8 Dependence of $\alpha = k_1[O_2]/k_3[M]$ value upon concentration of oxygen $[O_2]$ dissolved in oligomer

Oligomer	Value of α		
	$[O_2] = 1 \times 10^{-2}$ mol/l	$[O_2] = 2 \times 10^{-3}$ mol/l	$[O_2] = 3 \times 10^{-4}$ mol/l
dMA-EGA	40	8	≈ 1
teMA-tPA	35	7	≈ 1
hMA-PeA	30	6	≈ 1

Note. Typical values of $[O_2]$ in monomers for monomer saturation with oxygen under pressure of 100 kPa are 0.8×10^{-2} mol/l (25°C) and 1.0×10^{-2} mol/l (50°C) [2].

Physically, parameter α is the number of chain transfer events to oxygen per one event of chain propagation.

Only saturation of oligo(acrylates) with oxygen under pressure of 100 kPa ($[O_2] = 1 \times 10^{-2}$ mol/l) suppresses the chain propagation reaction practically completely ($\alpha = 30$–40), in the air atmosphere (at $[O_2]$ in oligomer 2×10^{-3} mol/l) $\alpha = 6$–8, and only reduction of $[O_2]$ to the value of 3×10^{-4} mol/l allows the chain propagation reaction to compete successfully with the reaction of chain transfer to oxygen ($\alpha \approx 1$).

In the context of the *layered model of TFRP of vinyl-type compounds*, it becomes possible to interpret the experimentally found dependence of kinetics of cross-linked polymer formation upon parameters regulating the rate of oxygen diffusion into film. In film, where the reaction with oxygen involvement takes places and where oxygen diffuses concurrently from the gas phase, the oxygen concentration gradient through film thickness appears, with the growth of $[O_2]$, from the substrate to the surface: $[O_2]^{(1)} < [O_2]^{(2)} < [O_2]^{(3)} \ldots$ due to $l_1 > l_2 > l_3 \ldots$, where 1, 2, and 3 are the layer numbers counting from the substrate. At a certain conversion degree, in the film layer adjacent to the substrate, $[O_2]$ should inevitably fall to a value at which the chain propagation reaction $\sim M^{\bullet} + M \xrightarrow{k_3} \sim MM^{\bullet}$ (3) starts competing successfully with the chain transfer reaction to oxygen $\sim M^{\bullet} + O_2 \xrightarrow{k_1} \sim MO_2^{\bullet}$ (1): increase in viscosity η resulting from accumulation of soluble polymers, i.e., products of oxidative polymerization, leads to the growth of $W_{\mathbf{O}_2}$ (gel effect), while W_D decreases because $D_{\mathbf{O}_2} = f(1/\eta)$. Such a situation occurs, first of all, in the layer adjacent to the substrate because the stationary $[O_2]$, the polymerization inhibitor, in it is always lower than in any of the upper-lying layers, and the viscosity of this layer grows most rapidly. Homo-polymerization develops as a process with positive feedback: polymerization acceleration from $[O_2]$ decrease results in increased polymer content in the layer and upgraded viscosity, which, in its turn, would retard oxygen diffusion into the layer still farther and accelerate polymerization. Then, a similar situation will be repeated in the second layer (the one above the first layer) and the TFRP front (originated in the near-the-substrate layer) would propagate layer by layer to the film surface. In this process, each layer successively passes through one and the same set of corresponding viscosity states, but with different, constantly growing degrees of conversions. In the context of the layered model, the TFRP kinetics should depend (with other factors being equal) upon parameters regulating oxygen concentration in each of the film layers: namely, film thickness, partial pressure of oxygen above the film, initiation rate, and oligomer oxidability.

Thus, it has been established that TFRP kinetics (namely, duration of induction period τ, polymerization rate W_p, and maximum yield of cross-linked polymer C_p) depends heavily upon film thickness l (Fig. 2.14) and partial pressure of oxygen in the gas phase P_{o_2} (Fig. 2.15). According to the forecast derived from the model, increase of l or decline of P_{o_2} results in the reduction of τ and growth of W_p and C_p. The layer-by-layer pattern of TFRP is verified directly: near-the-substrate layers contain a greater amount of cross-linked polymer and are less oxidized compared to film layers near its surface (Table 2.9).

According to the following criterion

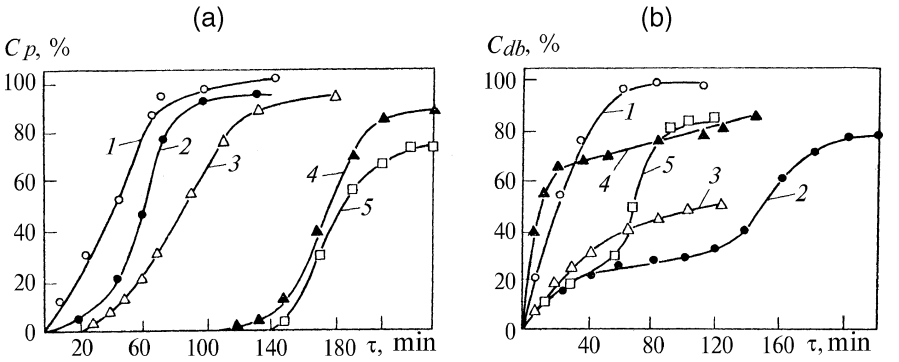

Fig. 2.14 Kinetic curves of cross-linked polymer formation (***a***) and consumption of double bonds (***b***) in oligo(acrylates) films.. (***a***) *1*, *2*, teMA-tPA, 80°C, film thickness 80 and 35 μm; *3*, *4*, *5*, dMA-EGA, 80°C, film thickness 80, 35, and 15 μm; (***b***) *1*, dMA-EGA, 100°C, film thickness 35 μm; *2*, *4*, teMA-tPA, 65°C, film thickness 35 and 80 μm; *3*, hMA-PeA, 65°C, 35 μm; *5*, teMA-tPA, 80°C, 35 μm

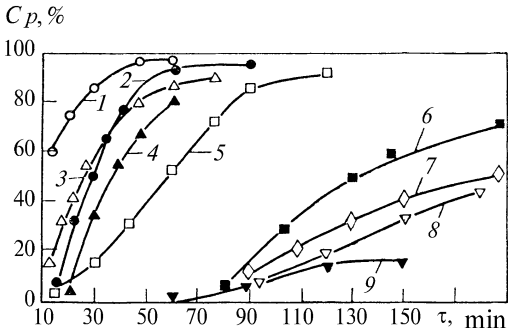

Fig. 2.15 Kinetic curves of cross-linked polymer formation in oligo(acrylates) films with thickness of 30 μm for various values of P_{O_2}: *1*, *3*,*4*, hMA-PEA, 65°C, 0, 21, and 100 kPa; *5*, *6*, *8*, teMA-tEA, 65°C, 0, 21, and 100 kPa; *2*, *7*, *9*, dMA-EGA, 100°C, 0, 21, and 100 kPa. Redox system composition, $(\text{mol/l}) \times 10^{-2}$: [DHHP] = 3.06, [cobalt naphtenate] = 1.07

$$W_{db}/W_{\mathbf{O}_2} = 1 - W_H/W_C \tag{2.5}$$

where W_{db}, WO_2, W_H, and W_C = rate of consumption of double bonds, rate of oxygen consumption, rate of homo-polymerization, and rate of copolymerization with oxygen, respectively.

Under given conditions, a cross-linked polymer is formed mainly due to the homo-polymerization reaction (Fig. 2.16). For example, at the maximum of curves $W_{db}/W_{\mathbf{O}_2} = f(\tau)$, when $C_p = 50$–80%, from 5 to 50 events $\sim M^{\bullet} + M \xrightarrow{k_3} \sim MM^{\bullet}$ accounted for 1 event $\sim M^{\bullet} + O_2 \xrightarrow{k_1} \sim MO_2^{\bullet}$. However, oxidative polymerization most likely prevails in the surface layer directly contacting with the air.

Table 2.9 Changes of acrylic (oligo)esters* and allylic** (oligo)ethers properties throughout their film thickness

Parameters	dMA-EGA*	teMA-tEA*	dAl-EGA**	teAl-tPA**
Content, % (by weight)				
Cross-linked polymer	63.9/95.1	61.5/92.5	46.7/57.0	58.4/65.3
Double bonds	8.1/7.1	50.3/49.8	28.7/23.3	50.0/44.5
Peroxide number, $gI_2/100\,g$	0.78/0.19	2.02/0.12	2.9/3.1	19.4/17.0
Acid number, mg KOH/g	22.7/5.1	0.88/0.74	18.3/22.9	29.5/25.8
Number of oxygen atoms attached by oligomer unit	2.08/1.24	3.34/2.64	2.12/1.90	3.25/3.15

Note 1. Numerator, upper layer; denominator, bottom layer.
Note 2. Total film thickness, 70 μm; thickness of upper and bottom layers, 15 μm each.
*, **Polymerization conditions: dMA-EGA, 100°C, 100 min; teMA-tEA, 80°C, 52 min; dAl-EGA, 100°C, 60 min; teAl-tPA, 80°C, 70 min.

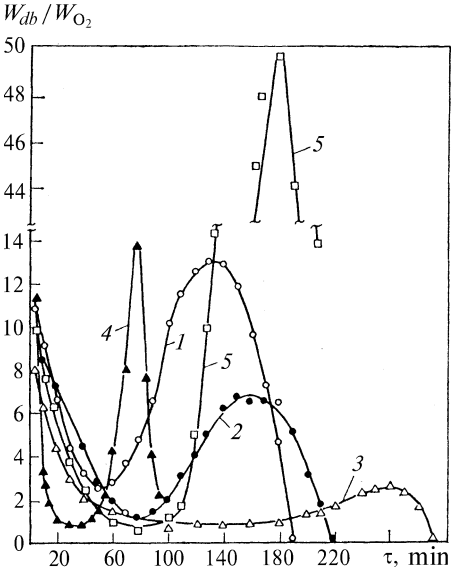

Fig. 2.16 Variation of W_{db}/W_{O_2} ratio for oligo(acrylates) polymerization: *1*, *2*, *3*, dMA-EGA, 80°C, film thickness 80, 35, and 15 μm; *4*, *5*, teMA-tPA, film thickness 35 μm; 80° and 65°C

Kinetic anomaly, that is, homo-polymerization in liquid films of oligo(acrylates) ($W_{db}/W_{O_2} = 5$–10) long before gel formation under the conditions of $W_{\mathbf{D}} > W_{\mathbf{O_2}}$, is discussed in Sect. 2.1.1.

However, specifics of TFRP in oligo(acrylates) films under oxygen diffusion conditions do not consist in layer-by-layer development of the process only. The authors found out that up to rather high-degree conversions, cross-linked polymers are formed from short-chain soluble polymers[5], and not directly as a result of oligomer polymerization. Soluble polymers are formed in the course of oligo(acrylates) polymerization in films in the air as the main product (before cross-linked polymer

[5] The term "soluble polymers" stands for non-cross-linked products of polyunsaturated compound polymerization.

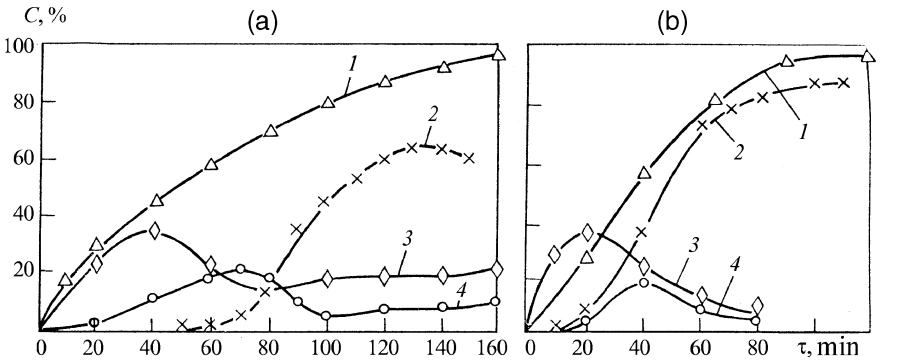

Fig. 2.17 Kinetic curves of dMA-EGA polymerization at 100°C in films with thickness of 35 (***a***) and 70 μm (***b***): *1*, conversion in terms of double bonds (C_{db}); *2, 3*, *4*, yield of cross-linked polymer and soluble polymers II and III (C_p, C_{II}, C_{III})

formation) during induction period of TFRP with duration τ, and as a part of sol fraction after the gel point is reached. In the presence of oxygen, the length of primary polymeric chains decreases approximately by two orders of magnitude, and under given polymerization conditions it should be about 10 oligomer units. This fact raises the stationary concentration of soluble polymers and shifts the beginning of gel formation into the area of high-degree conversions (C_{db} = 16–60% and τ = 20–100 min) (see Figs. 2.14 and 2.17). In terms of a set of properties [56], soluble polymers represent unsaturated oxidized compounds with polymerization degree $\overline{P}_p$ = 2–8 (low molecular fraction denoted as polymers II) and $\overline{P}_p > 8$ (higher molecular fraction, polymers III). Proton magnetic resonance spectroscopy (PMR) results indicate that chains of soluble polymers consist mainly of ∼MOOM∼ units and certain number of OK ∼MM∼ units.

The polymerizing ability of soluble polymers (the inverse values of induction period, formation rate, and maximum yield of cross-linked polymer could be taken as measures for this ability) changes in the following manner [59]:

- Polymers III are always characterized by greater polymerizing ability than polymers II
- Polymerizing ability of both polymers II and polymers III increases as molecular functionality of oligomers enhances
- The later after the beginning of oligomer polymerization the soluble polymers are extracted from films, the lower is their polymerizing ability

The entire set of results on kinetics of polymerization of oligo(acrylates) and their soluble polymers in films under oxygen diffusion conditions enabled the authors to propose and substantiate the following scheme of cross-linked polymer formation [59]:

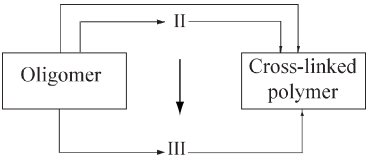

where II and III are soluble polymers of the II and III types.

It should be pointed out that the main direction of conversion is as follows: oligomer → polymer II → polymer III → cross-linked polymer. The following data could be provided in favor of this conclusion: within the limits of experimental error, the maximum value on accumulation curves for polymer II corresponds (in terms of time) to the highest rate of polymer III accumulation, while the maximum value of accumulation curves for polymer III corresponds to the highest rate of cross-linked polymer formation (Fig. 2.17).

During polymerization auto-acceleration, the relationship $dC_p/dC_{db} = q$ grows (Fig. 2.18). It means that until a certain degree of conversion, cross-linked polymer is formed mainly not from parent oligomer molecules, but from polymer III blocks that are becoming larger and larger in size.

A certain part of polymer III and cross-linked polymer is likely to be formed directly from the oligomer, which follows from the comparison of the rates of accumulation of these polymers and oligomer consumption. Such direction of TFRP appears to become prevailing for high-degree stages of conversion, in the studied cases, for transformation degrees with $C_p > 50$–60%.

Thus, the main kinetic specifics of TFRP of vinyl-type oligomers [such as oligo (acrylates)] in films under the conditions of diffusion of oxygen (which serves as polymerization inhibitor) are determined by layer-by-layer development of TFRP and by formation of cross-linked polymers, mainly from short-chain soluble polyunsaturated polymers that represent intermediate products of oligomer polymerization.

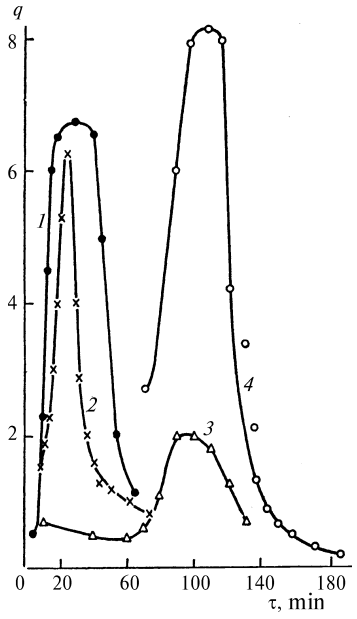

Fig. 2.18 Variation of parameter q for teMA-tPA polymerization (*1*, *3*, *4*) and hMA-PeA polymerization (*2*) in films of different thickness and at different temperatures: *1*, 80°C, 80 μm; *2*, 65°C, 35 μm; *3*, 65°C, 80 μm; *4*, 65°C, 35 μm

2.4.2 Allyl Compounds

2.4.2.1 Kinetic Features of Oxidative Polymerization of Allyl-Type Compounds in Films Under the Conditions of Oxygen Diffusion

These features have been mainly studied on oligomer ethers of allyl alcohol (propen-2-ol-1) (OEAl), diallyl(bis-ethylene glycol) adipate (dAl-EGA) and tetra allyl of (bis-trimethylolpropane) adipate (teAl-tPA), which had the identical structure of oligomer block with such oligo(acrylates) as dMA-EGA and teMA-tPA.

These circumstances enabled the authors to identify kinetic patterns of oxidation and oxidative polymerization common for compounds of vinyl and allyl types and made it possible to determine kinetic features of TFRP of oligomer allyl ethers, taking into account different reactive capacity of compounds of allyl and vinyl types in radical addition and radical substitution reactions. Experiments with OEAl in films were performed using a circulation volumometric unit [55] with the same redox system that was introduced in the same concentration as in the case with oligo(acrylates) (see Sect. 2.4.1).

Kinetic curves of oxygen absorption in dAL-EGA and teAl-tPA films (Fig. 2.19), in total, represent kinetics of oxidation and oxidative polymerization of OEAl, because, judging by results of experiments with monomer ethers of allyl alcohol [60], the oxidation and oxidative polymerization proceed as consecutive reactions.

In the case of oxidation of allylpropyl ether and allyl acetate within the range 35°–70°C, before conversion in terms of absorbed oxygen $C_{\mathbf{O}_2} \leq 0.5\%$, the amount of absorbed oxygen (with accuracy of 5%) corresponds to the amount of formed hydroperoxide with the structure $HOOCH_2–CH = CHOR$ [where R is $C_3H_7–$ or $CH_3C(O)–$], established using the PMR and infrared (IR) spectroscopy methods.

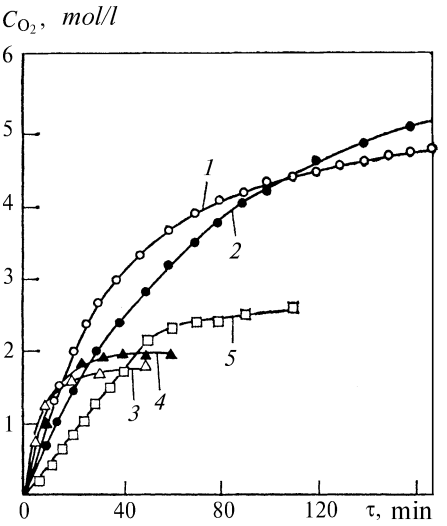

Fig. 2.19 Kinetic curves of oxygen absorption for OEAl polymerization in films with thickness of 35 μm at $P_{O_2} = 21$ kPa: *1* and *2*, dAL-EGA, 100° and 80°C; *3*,*4*, and *5*, teAl-tPA, 100°, 80°, and 65°C

Oxidation proceeds as a chain free-radical process according to the α-methylene mechanism [2 (p. 134)] with chain propagation stages:

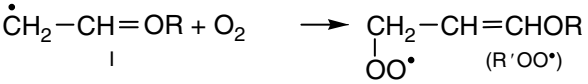

(1)

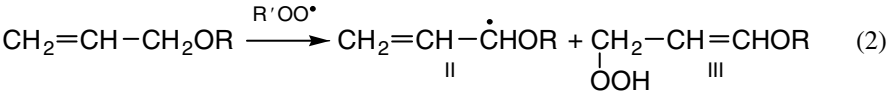

(2)

where R is C_3H_7— or $CH_3C(O)$—

Unsaturated hydroperoxide III (i.e., primary product of oxidation) is formed through homolytic elimination of allyl ether α-methylene by peroxide radical with subsequent isomerization of free radical II into radical I with the transfer of double bond and free valence migration. In this process, the double bond of unsaturated hydroperoxide III (not involved in oxidation) is activated as a result of π–*p* conjugation of π-electrons of the double bond with *p*-electrons of ether oxygen.

Oxidation of monomer allyl ethers to high conversions ($C_{\mathbf{O}_2} > 1$–2%, in block, at 50°C) results in the formation of polymer products with the following structure

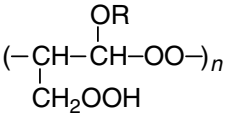

(where R: C_3H_7— or $CH_3C(O)$—), established using the PMR and IR-spectroscopy methods. This means that it is just unsaturated hydroperoxides III (not allyl ethers) that directly enter in the oxidative polymerization according to the mechanism characteristic for vinyl-type compounds $\sim M^{\bullet} + O_2 \rightarrow \sim MO_2^{\bullet}(1)$, $\sim MO_2^{\bullet} + M \rightarrow \sim MOOM^{\bullet}(2)$ (where M: $HOOCH_2CH{=}CHOR$).

Thus, interaction of monomer ethers of allyl alcohol with oxygen for low-degree conversions proceeds in two stages: in the form of consecutive reactions of co-oxidation and oxidative polymerization.

The autocatalytic character of the process of OEAl interaction with oxygen and the dependence of this process upon conditions and oligomer structure (Figs. 2.19, 2.20 and 2.21) is obvious. The influence of structure is manifested in the fact that, with other factors being equal, limiting conversions $C_{\mathbf{O}_2 \lim}$ decrease as molecular functionality enhances. Most probably the autocatalysis is provided both by degenerate branching on hydroperoxides with participation of cobalt naphthenate and by inhibition of quadratic termination of chain on polyperoxide radicals accompanied by gel-effect development.

However, experimental data indicate that specifics of OEAl oxidation and OEAl oxidative polymerization are not exhausted by trivial development of autocatalysis. The authors also established that the kinetics of OEAl interaction with oxygen diffusing into film depends heavily upon film thickness and partial pressure of oxygen $P_{\mathbf{O}_2}$ in the gas phase (Figs. 2.20 and 2.21). Similar to the oxidative polymerization of oligo(acrylates), the autocatalysis degree and limiting conversions $C_{\mathbf{O}_2 \lim}$ are inversely dependent upon film thickness, and they increase as $P_{\mathbf{O}_2}$ grows.

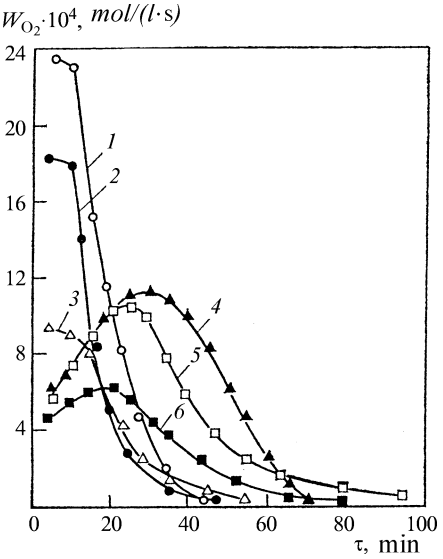

Fig. 2.20 Dependence of W_{O_2} upon duration of teAl-tPA polymerization in films of different thickness at $P_{O_2} = 21$ kPa: *1*, *2*, and *3*, 80°C, 15, 35, and 70 μm; *4*, *5* and *6*, 65°C, 15, 35 and 70 μm

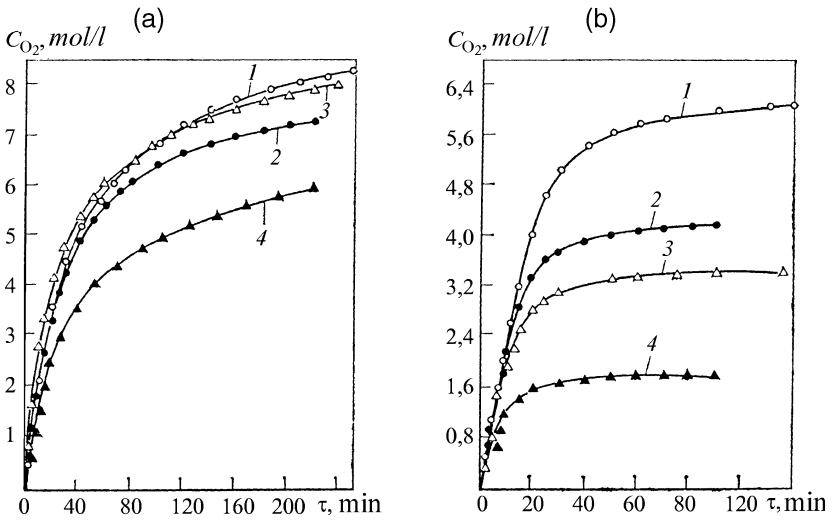

Fig. 2.21 Kinetic curves of oxygen absorption for dAL-EGA polymerization at 100°C (***a***) and teAl-tPA at 80°C (***b***) for different values of Po_2: ***a*** *1*, *2*, 15 μm, 100 and 21 kPa; *3*, *4*, 35 μm, 100 and 21 kPa; ***b*** *1*, *2*, 15 μm, 100 and 21 kPa; *3*, *4*, 35 μm, 100 and 21 kPa

In a number of cases, coincident sections of kinetic curves are observed for films with different thickness and different values of Po_2, and the length of these sections increases as the value of Po_2 goes up. These regularities were interpreted within the framework of the *layered model for oligo(acrylates) oxidative polymerization* (see Sect. 2.4.1) that give us grounds to extend the layered model on the process of OEAl oxidation and OEAl oxidative polymerization.

2.4.2.2 Kinetic Features of TFRP of Allyl-Type Compounds in Films Under Oxygen Diffusion Conditions

These features for oligomer allyl ethers and oligo(acrylates) are very different. In the case of oligo(acrylates), TFRP kinetics depends upon parameters regulating the rate of oxygen diffusion into film as follows: duration of induction period τ declines as film thickness l increases and partial pressure of oxygen P_{O_2} decreases, while the formation rate W_p and maximum yield of cross-linked polymer C_pC_{lim} increase (see Figs. 2.14 and 2.15). In the absence of oxygen, with other conditions being equal, the oligo(acrylates) polymerization proceeds without induction period ($\tau = 0$), with the highest W_p and $C_p \geq 95\%$ (see Fig. 2.15). In contrast, in the case of OEAl polymerization in films, the induction period duration grows as the value of P_{O_2} decreases and the value of l increases, while formation rate and maximum yield of cross-linked polymer go down (Fig. 2.22). In the absence of oxygen, with other conditions being equal, the OEAl polymerization proceeds at minimal values of W_p and C_p. For instance, in teAl-tPA films at 80°C when switching over from polymerization in the air to polymerization in vacuum, the induction period duration grows from 20 to 35 min, and C_p falls from 85 to 20% (curves *3* and *3′* in Fig. 2.22a); polymerization in vacuum stops when approximately 70% of double bonds are still unconsumed (curves *2* and *2′* in Fig. 2.22b).

It is highly probable that OEAl oxidation by oxygen diffusing into the film with production of hydroperoxides and concurrent activation of double bonds is a necessary precondition for TFRP of these oligomers.

Indeed, the authors failed to interpret the above-indicated features of TFRP in OEAl films in the context of the layered model without using such an assumption.

Fundamental notions of the layered model of TFRP for allyl-type compounds are as follows. At the moment of time t_1, with the onset of oligomer oxidation, diffusion

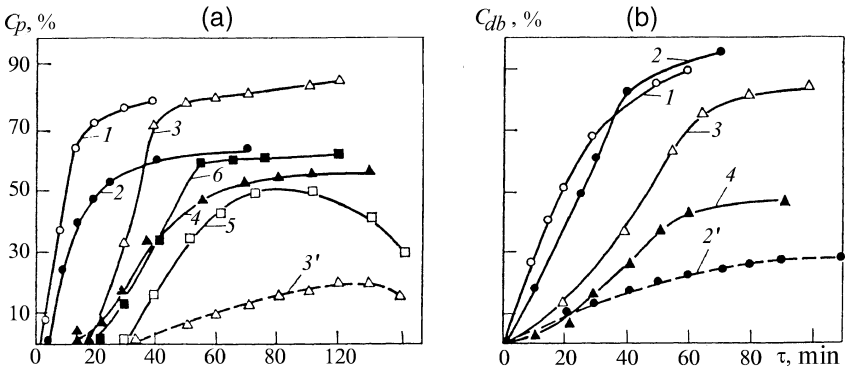

Fig. 2.22 Kinetic curves of cross-linked polymer formation (**a**) and consumption of double bonds (**b**) in OEAl films in the air (— —) and in vacuum (----): (***a***) *1*, *2*, teAl-tPA, 100°C, 35 and 70 μm; *3*, *3′*, *4*, teAl-tPA, 80°C, 35 and 70 μm; *5*, *6*, dAL-EGA, 100°C, 35 and 70 μm; (***b***) *1*, dAL-EGA, 100°C, 35 μm; *2*, *2′*, teAl-tPA, 80°C, 35 μm; *3*, *4*, teAl-tPA, 65°C, 35 and 70 μm

flow of oxygen is generated from the gas phase into the film and gradient $[O_2]$ is established, with growing, layer after layer $[O_2]$ from the substrate to the film surface $[O_2]^{(1)} < [O_2]^{(2)} < [O_2]^{(3)} < \ldots$, where 1, 2, 3 is a layer number counting from the substrate. Variation of $[O_2]$ in the i-th film layer is determined by the difference between oxygen consumption rate $W^i_{O_2}$ and oxygen diffusion rate W^i_D into the i-th layer. With high enough thickness of film l, in a layer adjacent to the substrate, from the very beginning of oxidation t_1 $W^{(1)}_D$ may turn out to be much lower than $W^{(1)}_{O_2}$, where index 1 denotes the layer number. Then, by the moment in time t_2, hydroperoxides HP with concentration $[HP]^{(1)}$ would accumulate in this layer and certain amount of oxygen with concentration $[O_2]^{(1)}$ would be left. The following inequality would be a condition for the beginning of polymerization (not inhibited by O_2) in any layer

$$[HP]/[O_2] > ([HP]/[O_2])_{cr} \tag{2.6}$$

which follows from the mechanism of oxidation, oxidative polymerization, and polymerization of unsaturated compounds, when these processes are initiated by hydroperoxides produced during oxidation [4]. Depending on oxidation conditions (temperature, P_{O_2}, initiation rate W_I, length of oxidation chains), by the moment in time t_2, in the near-the-substrate layer, into which oxygen does not diffuse, either condition $[HP]^{(1)}/[O_2]^{(1)} > ([HP]/[O_2])_{cr}$ is fulfilled and polymerization starts, or almost the entire amount of oxygen would be consumed in it without producing such amount of HP that is sufficient for polymerization initiation. Then this layer, where $[HP]^{(1)}/[O_2]^{(1)} < ([GP]/[O_2])_{cr}$, will be left nonpolymerized.

In this situation, if the film is thick enough, there always is an i-th layer located closer to the surface, into which oxygen inflows due to diffusion at rate W^i_D that is not significantly higher than oxidation rate $W^i_{O_2}$; therefore, [HP] would definitely reach the stationary concentration $[HP]_{st}$, when the oxygen consumption rate is maximum and does not depend upon $[O_2]$. At the same time, the oxygen diffusion rate into this layer will continuously decline due to viscosity changes caused by accumulation of polymer products of oxidative polymerization with corresponding decrease of $[O_2]^i$. It should be pointed out here that oxidative polymerization most likely proceeds only in conjugated double bonds formed as a result of hydroperoxide oxidation of OEAl without involving nonconjugated double bonds of nonoxidized molecules of oligomers. Hence, starting from a certain moment in time, condition $[HP]^i/[O_2]^i > ([HP]/[O_2])_{cr}$ will be certainly fulfilled in the i-th layer and polymerization would start. In layer $(i+1)$ located above the i-th layer, [HP] reaches $[HP]_{st}$, somewhat earlier than in the i-th layer, but $[O_2]^{i+1} > [O_2]^i$ due to $l_i > l_{i+1}$. In the $(i+1)$-th layer, the viscosity changes required for fulfillment of polymerization beginning conditions would occur at a more advanced stage of oxidation and oxidative polymerization. The increased viscosity zone (extending from the i-th layer upward) will diminish the oxygen diffusion rate, thus facilitating the fulfillment of polymerization process condition in the $(i+1)$-th layer. Then, the same situation will be repeated in the $(i+2)$-th layer and then, in turn, in all upper layers, with each of them passing successively through one and the same set of corresponding viscosity states, but at different, steadily growing degrees of conversion. Thus, after the front

of polymer transformations has been generated in the i-th layer, it would start extending upward. Extension of this front downward would be attenuated very soon, because the dense film of the i-th layer would hinder the access of oxygen to lower layers, where the condition (2.6) is not fulfilled in any case, $[HP] < [HP]_{st}$; besides, the deeper the layer is, the lower is [HP]. Nonpolymerized lower-located layers will be "immured," in other words, excluded from the polymerization process.

If by the moment in time t_2, condition $[HP]^{(1)}/[O_2]^{(1)} > ([HP]/[O_2])_{cr}$ is fulfilled in the layer adjacent to the substrate, then, in accordance with the mechanism described above, it would be successively fulfilled in the second, third, and each of the upper-located film layers, but at increasingly higher degrees of conversion. The front of polymer transformations (i.e., viscosity changes) would extend from the near-the-substrate layer (as it does from the i-th layer) to the film surface and no unpolymerized ("immured") layers would be left in the film.

Hence, for each of the specific conditions upon which [HP] and $[O_2]$ depends, namely, temperature, values of P_{O_2}, D_{O_2}, and W_I, oxidation chain length, a critical film thickness l_{cr} exists, which is characterized by the fact that in films with $l < l_{cr}$, not-oxygen-inhibited polymerization would not proceed at all, whereas in films with $l > l_{cr}$ it would proceed only partially to a depth that is approximately equal to l_{cr}, counting from the film surface. In films with thickness $l > l_{cr}$, such TFRP parameters as $1/\tau W_p$, and C_{lim} would depend directly upon partial pressure of oxygen P_{O_2} above the film and film thickness, and these parameters, in the end, regulate $[O_2]$ and [HP] in each film layer.

Indeed, in OEAl films with thickness of 35–70 μm, the induction period duration τ declines under oxygen diffusion conditions, while rate W_p and limiting conversion of cross-linked polymer C_{lim} grows with increasing P_{O_2} and reducing film thickness (Fig. 2.22). With the distance from the surface of the i-th layer, where polymerization is originated, being equal for two films with different thickness, the part of the film (cut off from oxygen access by this layer) is larger in the thicker film. This leads to a decrease of measured integral values W_p and C_p (averaged throughout the film volume) because condition (2.6) is not fulfilled in the "immured" layers and polymerization does not take place. In terms of its influence on TFRP kinetics, the decrease of $P_{\mathbf{O}_2}$ is equivalent to film thickness growth. The authors managed to identify nonpolymerized film layers "immured" near the substrate (and forecast by the layered model of TFRP) with polymerization of *cis*-oligobutadiene, the allyl-type oligomer (Table 2.10).

Table 2.10 Changes of features in *cis*-oligobutadiene films throughout their thickness

Indices	Upper layer	Lower layer
Cross-linked polymer content, %	25.7	0.0
Double bonds content, %	59.2	90.0
Peroxide number, g I_2/100 g	15.6	3.8
Acid number, mg KOH/ g	33.2	1.5
Oxygen content, %	7.01	2.07

Note. Total film thickness, 70 μm; thickness of upper and lower layers, 15 μm each; polymerization temperature, 20°C; exposure time, 4 h.

The authors also obtained experimental data that are indicative of the presence of films with thickness $l < l_{cr}$, in which OEAl polymerization (not inhibited by oxygen) does not take place at all. For instance, for dAL-EGA at 100°C, $W_I = 2 \times 10^{-5}$ mol/(1 · s), $P_{O_2} = 21$ kPa (in the air), a cross-linked polymer is not formed at all in films with thickness 15 μm, despite the fact that more than 95% of double bonds have reacted. Probably for this oligomer, the value of $l_{cr} > 15$ μm under given conditions.

This assumption could be substantiated in the following way. For polymerization in films under oxygen diffusion conditions, the number of cross-links per film volume unit is determined by the ratio of rates of the following competing polymerization reactions: $\sim M^{\bullet} + M \rightarrow \sim MM^{\bullet}$ (3) with formation of one cross-link per each reacted double bond and oxidative polymerization: $\sim M^{\bullet} + O_2 \xrightarrow{k_1} \sim MO_2^{\bullet}$ (1) and $\sim MO_2^{\bullet} + M \xrightarrow{k_2} \sim MOOM^{\bullet}$ (2), with the number of cross-links being less than one for each reacted double bond due to destructive transformations for bonds —COOC —. Under identical conditions in terms of temperature, film thickness and P_{O_2}, dAL-EGA polymerization proceeds with much higher contribution of reactions (2.1) and (2.2) versus dMA-EGA polymerization (Figs. 2.23 and 2.16) and, hence, dAL-EGA films contain a considerably lower amount of cross-linked polymer than dMA-EGA films (Table 2.9). Polymers of upper layers of OEAl and oligo(acrylates) films, judging by diminished content of cross-linked polymer versus their lower layers (Table 2.9), are subjected to oxidative destruction the most. Probably a cross-linked polymer is formed in the upper layers of oligomers of vinyl and allyl types with thickness $l > l_{cr}$ mainly because of oxidative polymerization In the limiting case, with $l < l_{cr}$ under the conditions when polymerization process is represented by oxidative polymerization only, while oxidative destruction is developed quite considerably, a cross-linked polymer is not formed at all in all layers of the dAL-EGA film.

However, specifics of TFRP in OEAl films under oxygen diffusion conditions are not confined to layer-by-layer development of the process. The authors found out that a significant part of cross-linked polymers is formed not directly during polymerization of oligomers, but from short-chain soluble polyunsaturated polymers that represent intermediate products of the TFRP process. Soluble polymers

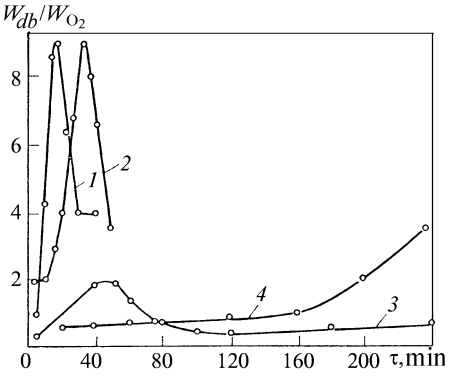

Fig. 2.23 Variation of W_{db}/W_{O_2} ratio for OEAl polymerization. *1*, teAl-tPA, 100°C, 70 μm; *2*, teAl-tPA, 80°C, 70 μm; *3*, dAL-EGA, 100°C, 15 μm; *4*, dAL-EGA, 80°C, 35 μm

are formed during OEAl polymerization as the main product before the beginning of TFRP (during TFRP induction period τ) and as a part of sol-fraction after reaching the gel point. Oxidative polymerization by double bonds activated by π–p conjugation under the conditions of strongly developed chain transfer to oligomer by α-methylene groups inevitably results in quite short-chain polymers, the polymerization degree of which $\overline{P}_p$ increases slightly (in average, up to $\overline{P}_p \approx 10$) due to homo-polymerization. The formation of just short-chain polymers upgrades their stationary concentration and shifts the beginning of gel formation to the area of higher conversions ($C_{db} = 20$–50%, $\tau = 20$–30 min; Figs. 2.22 and 2.24).

In terms of a set of properties [2 (p. 120)], soluble OEAl polymers are unsaturated compounds with polymerization degree $\bar{P}_p = 2$–8 (low molecular fraction denoted as polymers II) and $\bar{P}_p > 8$ (higher molecular fraction, polymers III). PMR results show that the ratio of ∼MOOM∼ and ∼MM∼ units in chains of soluble dAL-EGA and teAl-tPA polymers lies in the range from 4:1 to 3:1, which indicates that in addition to oxidative polymerization, homo-polymerization also proceeds under the above-described conditions ($t = 65°$–$100°$C, $P_{O_2} = 21$kPa, $l = 35$–70 μm).

Polymerizing capacity of soluble polymers in films was studied under the conditions taken for parent oligomers [2 (p. 124); 61]. The obtained results could be summarized as follows:

- Polymerizing capacity that was estimated based on polymerization rate and limiting yield of cross-linked polymers is always higher for polymer III vs. polymer II.
- Polymerizing capacity of polymers II and III grows as molecular functionality of oligomer enhances.
- The later from the beginning of oligomer polymerization that soluble polymers are isolated from films, the lower is their polymerizing capacity.

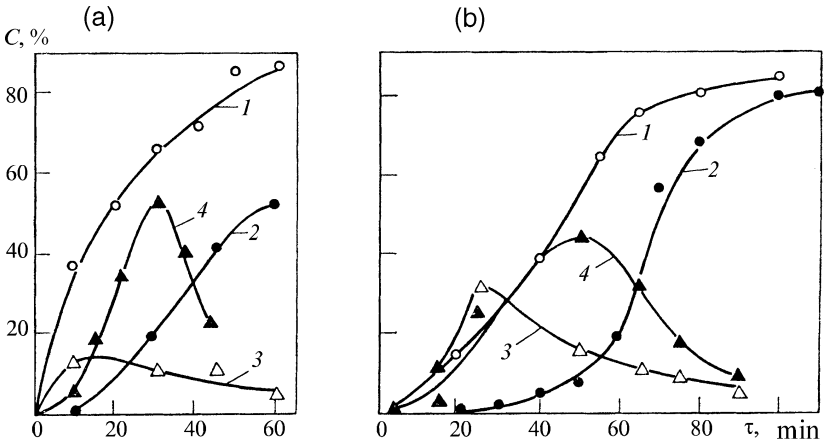

Fig. 2.24 Kinetic curves for dAl-EGA polymerization at 100°C(**a**) and teAl-tPA polymerization at 65°C(**b**) in films with thickness 35 μm: *l*, double-bond conversion (C_{db}); *2*,*3*,*4*, yield of cross-linked polymer and soluble polymers II and III (C_p, C_{II}, C_{III})

A total set of results on kinetics of OEAl and their soluble polymer polymerization in films under oxygen diffusion conditions gives grounds for us to consider the following direction of polymerization transformations as the main one: oligomer → polymer II → polymer III → cross-linked polymer. The following data could be provided in favor of this conclusion:

- Within the limits of experimental error, the maximum value on accumulation curves for polymer II corresponds (in terms of time) to the highest rate of polymer III accumulation, while the maximum value on accumulation curves for polymer III corresponds to the highest rate of cross-linked polymer formation (see Fig. 2.24).
- During the polymerization auto-acceleration period, polymer yield per each reacted double bond $q = dC_p/dC_{db}$ (Fig. 2.25) increases; this means that until a certain degree of conversion is reached, the cross-linked polymer is formed mainly not from molecules of parent oligomer, but from polymer III volumes that are becoming larger and larger in size.

Probably a certain part of polymer III and cross-linked polymer is still formed directly from oligomer during high-degree conversions with $C_p \geq 50\%$. On the whole, the scheme proposed earlier for oligo(acrylates) polymerization could be also applied for the formation of OEAl polymers (see Sect. 2.4.1).

Thus, main kinetic features of TFRP for oligomer allyl ethers in films under oxygen diffusion conditions are determined by the layer-by-layer development of TFRP and formation of cross-linked polymers mainly from short-chain soluble polyunsaturated polymers that represent intermediate products of polyunsaturated oligomer polymerization. It should be also pointed out here that the mechanisms of layer-by-layer development of TFRP and causes of formation of soluble polymers for OEAl and oligo(acrylates) (as compounds of allyl and vinyl types) are totally different (see Sects. 2.4.1 and 2.4.2).

The role of oxygen (diffusing into the film) in TFRP of compounds of allyl type is also fundamentally different from its role in TFRP of vinyl-type compounds. For OEAl and other allyl-type compounds with double bonds that are not so active in radical addition reactions and with strongly developed reaction of chain transfer on oligomer, oxidation is a necessary condition for TFRP development.

Oxidative polymerization and polymerization (which are responsible for TFRP) are most likely initiated mainly by hydroperoxides, which are formed during OEAl

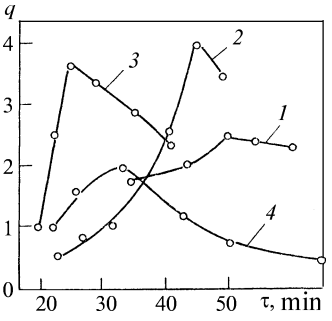

Fig. 2.25 Variation of parameter q during dAL-EGA polymerization (*1*, *2*) and teAl-tPA polymerization (*3*, *4*) in films of different thickness and at different temperatures: *1* and *2*, 100°C, 35 and 70 μm; *3* and *4*, 80°C, 15 and 35 μm

oxidation caused by oxygen diffusing into the film. In contrast, TFRP of vinyl-type compounds [including oligo(acrylates)] with double bonds that are highly reactive in radical addition reactions, the oxygen diffusing into the film is, first of all, an inhibitor, and oxidation is just an inevitable secondary process.

2.5 Three-Dimensional Free-Radical Polymerization as a Tool for Macromolecular Design of Cross-Linked Polymers

Actually, a final goal of any kinetic or structural and physical study in the field of polymers is gaining basic data for macromolecular design. These data include kinetic regularities, mechanism of macromolecule formation process, and patterns of formation of supermolecular structures regulating properties of polymer solids (materials). In the case of linear (non-cross-linked) macromolecules, the final structure of polymer solids is influenced both by polymerization process parameters regulating molecular mass characteristics of macromolecules and by conditions of supermolecular structure formation process, which include purposeful technological action, such as thermal, mechanical (pressing, calendaring, rolling, etc.), and introduction of modifying additives. In the case of cross-linked (linked) and especially highly cross-linked polymers, the polymerization process parameters exert decisive influence upon the formation of polymer solids and, hence, final polymer properties, because opportunities for special technological action on these are dramatically limited by to infusibility, insolubility, and weakly expressed relaxation capacity of highly cross-linked polymers.

Macromolecular design of cross-linked polymers (that are TFRP products) is implemented based on results of fundamental studies that enable determining specifics of kinetic regularities and TFRP mechanism, the main peculiarity of which consists in microheterogeneity (see Chaps. 1 and 2). To use these results as an effective tool for macromolecular design, they should be transformed into a mathematical (computer) TFRP model. Currently existing TFRP models can be classified into two groups: the microheterogeneous model and homogenous models.

The *microheterogeneous model*, which is based on kinetic interpretation of simplified concepts of the microheterogeneous mechanism of TFRP, was developed from the end of the 1970s to the beginning of the 1980s [3]. In summary, it could be presented as follows. Microgel particles, operating in the mode of self-contained micro-reactors, are approximated with spheres of averaged radius r. It is assumed that the polymerization process is localized in the peripheral layer of such sphere (with thickness h that does not change as degree of conversion increases) (see Fig. 1.8). Computations showed that the number of micro-reactors during transformation is virtually constant, so the growth in the conversion degree of occurs due to the increase of r. After r reaches a value at which spheres begin contacting each other, their loose peripheral layers (playing roles of effective reactors) partially overlap, and their cores, consisting of highly cross-linked polymers with limiting conversion and, therefore, incapable of mutual penetration, are packed as a tetragonal or (which is less probable) a hexagonal structure. Cavities of the structure

made of spheres (more precisely, internal near-the-surface layer of these cavities with thickness h) serve as the place of polymerization process localization (reaction zone) at this stage. With sufficiently high conversion, the spherical shape of these cavities (with average radius r') is assumed. It is obvious that in the course of subsequent polymerization the value of r' declines.

Within the framework of such a model (the percolation model), the constants of rates of all elementary acts (initiation, propagation, termination) do not change with conversion changes because, during polymerization, conditions in the reaction zone (in loose near-the-surface layers over dense highly cross-linked polymer) remain the same, and only the total volume of the reaction zone changes: at first it grows (until the moment when spheres come into contact), and then declines. Correspondingly, the overall (experimentally observed) reduced rate of polymerization $W/[\mathrm{M}]$ at first increases (auto-acceleration stage), and then decreases (auto-deceleration). Both stages in this case could be described with simple mathematical expressions:

Auto-acceleration:

$$W = W_0\left(1 - \frac{C}{C_{\lim}}\right) + W_r(4\pi N)^{1/3}h\left(\frac{3C}{C_{\lim}}\right)^{2/3} \tag{2.7}$$

where W_0 and W_r = polymerization rates in the initial reaction medium and in spherical layers with thickness h; C = current conversion; $C_{\lim}$ = limiting conversion; and N = concentration of spherical micro-reactors (microgel particles, grains).

Auto-deceleration:

$$W = W_0\left(1 - \frac{C}{C_{\lim}}\right) + W_r(4\pi N)^{1/3}h3^{2/3}\left(1 - \frac{C}{C_{\lim}}\right)^{2/3} \tag{2.8}$$

However, an interval between auto-acceleration and auto-deceleration cannot be described with such simple relationships.

The number of micro-reactors (microgel particles) formed in the reaction system reaches constant value $N_{\lim}$ already at early TFRP stages (with $C < 1\%$); it depends on both kinetic parameters and reaction conditions.

In the absence of inhibiting additives:

$$N_{\lim} = \frac{W_{\mathrm{I}}k_{ter}}{(f-1)k_{\mathrm{pr}}^2[\mathrm{M}]_0} \tag{2.9}$$

where W_{I} = initiation rate; f = monomer functionality; and $[\mathrm{M}]_0$ = initial monomer concentration.

In the presence of inhibitor X, the value of $N_{\lim}$ is derived from Eq. (2.2), in which k_{X} = constant of acceptance rate of radical-chain carriers.

Equations (2.2, 2.7, 2.8, and 2.9) show how one can control TFRP kinetics and morphology of highly cross-linked polymers being formed. For instance, increasing W_{I} or/and introducing additives of inhibitor X makes it possible to transform a large-grain structure into a fine-grain one. An advantage of this model consists in the fact that it takes the microheterogeneous pattern of TFRP into account.

Homogeneous mathematical (computer) models imply more complicated formulas [42–44, 62–64]. Elementary TFRP acts (initiation, chain propagation, and termination) are assumed to proceed under the conditions of diffusion control. Therefore, effective values of their rate constants are dependent in certain manner upon conversion and vary in the course of polymerization. Type of functions $k = f(C)$ depends on selection of a particular physical model of diffusion control of elementary acts: either the Smolukhovsky one, or within the framework of the free volume theory, or with involvement of concepts on "reaction" diffusion. It should be pointed out that certain physical constants remain undefined and subsequently (i.e., during comparison of calculation results with experimental data) they play the role of adjustable parameters. From the applied science standpoint, such a semiempirical theory has certain advantages: obtained formulas are applicable for forecasting macromolecule design, but only under limited conditions because of the empirical character of parameters.

The most developed model is the one [62] where expressions for constants of elementary act rates are obtained in the following form:

$$k_{\text{pr}} = \frac{k_{\text{pr0}}}{1 + \exp[A_{\text{pr}}(1/\nu - 1/\nu_{\text{av}})]} \tag{2.10}$$

$$k_{\text{ter}} = \frac{k_{\text{pr0}}}{1 + \{R_{\text{d}} k_{\text{pr}}[\text{M}]/k_{\text{ter0}} + \exp[-A_{\text{ter}}(1/\nu - 1/\nu_{\text{av}})]\}^{-1}} \tag{2.11}$$

Here k_{pr0} = true kinetic propagation constant, i.e., value of k_{pr} in the absence of diffusion control; A = parameter determining how fast the diffusion-controlled kinetic constant decreases with growing hindrances for diffusion; V = average partial free volume of the system; v_{cr} = critical free volume for chain propagation reaction determined as a value, with which $k_{\text{pr}} = (1/2)k_{\text{pr0}}$; $R_{\text{d}}k_{\text{pr}}[\text{M}]$ = member representing the contribution of the "reaction diffusion" mechanism; [M] = instantaneous concentration of double bonds; and R_{d} = a parameter characterizing "reaction diffusion."

To calculate the partial free volume for a given conversion, it is necessary to know six parameters of a material: monomer and polymer density (ρ_m and ρ_{p}), their glass-transition temperatures (T_{gm} and T_{gp}), and the difference of expansion coefficients in high-elastic and glass states (α_m and α_p). Parameter R_d is determined [40] based on results of nonstationary experiments (post effect) as follows:

$$R_{\text{d}} = \frac{k_{\text{ter}}}{k_{\text{pr}}[\text{M}]} \tag{2.12}$$

Such an approach does not take microheterogeneity of the reaction medium into account (in an explicit form), and it is little different from known gel effect theories developed for the case of linear polymerization of conventional (monofunctional) vinyl monomers in high-viscosity media [11]. Trivial kinetic regularities of TFRP (autocatalysis at early stages, auto-deceleration at high-degree conversions, type of dependence W/[M] upon initiation rate with fixed values of C), as well as results of nonstationary kinetic measurements of "elementary" (but, actually, effec-

tive) constants of chain propagation rates and chain termination rates agree quite satisfactorily with results obtained through the use of models that are based on dependence of diffusion-regulated constants of rates upon the reaction medium state determined by conversion.

However, during TFRP, nontrivial processes and phenomena (described in detail and analyzed in monographs [3, 5], as well as presented in Chaps. 1 and 2) are observed, which cannot be interpreted based on homogenous models with constants $k = f(C)$: that is why a microheterogeneous model of TFRP was developed.

It is obvious that both models—a homogenous model and a microheterogeneous one—represent extreme (limiting) cases of TFRP. Actually, the TFRP microheterogeneity is most expressed for oligomers with short and/or hard oligomer blocks in the case of polymerization with low rates of initiation (no higher than $10^{-7}\,\mathrm{mol}\cdot\mathrm{l}^{-1}\cdot\mathrm{s}^{-1}$). For oligomers with long and/or flexible blocks or in the case of polymerization with very high initiation rates (above 10^{-6}–$10^{-5}\mathrm{mol}\cdot\mathrm{l}^{-1}\cdot\mathrm{s}^{-1}$), microheterogeneity becomes less expressed. Recently when conducting TFRP in the "living" chain mode, during copolymerization with appropriately selected comonomers, as well as during polymerization in the mode of formation of very short chains (inhibition, chain transfer, catalytic chain transfer), researchers managed to minimize sources of heterogeneity origination to such an extent that for these cases the homogeneous model of radical polymerization is quite applicable.

We would like to especially emphasize here that considerable efforts by researchers are focused on issues of computer modeling of TFRP [41–44, 62–64]. Rapid development of this research area is important for extending the opportunities for macromolecular design of cross-linked polymers.

References

1. Berlin AA, Kefeli TYa, Korolev GV (1967) Poly-esteracrylates. Nauka, Moscow
2. Mogilevich MM (1977) Oxidative polymerization in film-formation processes. Khimia (Chemistry), Leningrad
3. Berlin AA, Korolev GV, Kefeli TYa, Sivergin YuM (1983) Acrylic oligomers and materials on the acrylic oligomers. Khimiya, Moscow (in Russian)
4. Mogilevich MM, Pliss EM (1990) Oxidation and oxidative polymerization of unsaturated compounds. Khimia (Chemistry), Moscow (in Russian)
5. Korolev GV, Mogilevich MM, Golikov IV (1995) Cross-linked polyacrylates: micro-heterogeneous structures, physical networks, deformation-strength properties. Khimiya, Moscow (in Russian)
6. Korolev GV, Berlin AA, Kefeli TYa (1962) Vysokomolek Soedin **4**:1520–1527 (in Russian)
7. Kefeli TYa, Korolev GV, Filippovskaja YuM (1961) J Polym Sci **52**:169–177
8. Korolev GV, Berezin MP (1997) Vysokomolek Soedin A **39**:242–249 (in Russian)
9. Korolev GV, Boichuk IN, Mogilevich MM et al (2001) Vysokomolek Soedin A **43**:713–721 (in Russian)
10. Bagdasaryan XS (1966) Radical polymerization theory. Nauka, Moscow (in Russian)
11. Gladyshev GP, Popov VA (1974) Radical polymerization at deep conversion degrees. Nauka, Moscow (in Russian)

12. Tvorogov NN (1967) Synopsis of thesis for Ph.D. degree in chemistry. Institute of Chemical Physics of the USSR Academy of Science, Moscow (in Russian)
13. Plate NA, Ponomarenko AG (1974) Vysokomolek Soedin A **16**:2635–2645 (in Russian)
14. Lipatov YuS, Nesterov A.S., Gritsenko TM, Veselovskiy RA (1971) Reference book on chemsitry of polymers. Naukova Dumka, Kiev (in Russian)
15. Berlin AA, Samarin EF (1969) Vysokomolek Soedin B **9**:530–533 (in Russian)
16. Berlin AA, Tvorogov NN, Korolev GV (1966) Dokl Akad Nauk **170**:1073–1076 (in Russian)
17. Berlin AA, Tvorogov NN, Korolev GV (1966) Izv AN SSSR Khimia No. **1**:193 (in Russian)
18. Mogilevich MM, Sukhanov GA, Korolev GV(1975) Vysokomolek Soedin A **17**:2487–2492 (in Russian)
19. Semenov NN (1960) Chemistry and technology of polymers 1960, No. **7**:8196–198 (in Russian)
20. Plate NA, Shibayev VP (1980) Comb polymers and liquid crystals. Khimiya, Moscow (in Russian)
21. Korolev GV, Perepelitsyna EO (2000) Dokl Akad Nauk **371**:488–492 (in Russian)
22. Korolev GV, Perepelitsyna EO (2001) Vysokomolek Soedin A **43**:774–783 (in Russian)
23. Semenov NN (1958) Certain issues of chemical kinetics and reactive capacity. Publishing House of USSR Academy of Science, Moscow (in Russian)
24. Salem L (1985) Electrons in chemical reactions. Mir, Moscow (Russian translation)
25. Minkin VI, Simkin Vya, Minyayev RM (1986) Quantum chemistry of organic compounds: reaction mechanisms. Khimiya, Moscow (in Russian)
26. Korolev GV, Ilyin AA, Mogilevich MM et al (2002) Izv Vuz Khim Khim Tekh **45**:33–38
27. Korolev GV, Ilyin AA, Mogilevich MM et al (2003) Vysokomolek Soedin A **45**:883–890 (in Russian)
28. Korolev GV, Mogilevich MM, Ilyin AA (2002) Association of liquid organic compounds. Mir, Moscow (in Russian)
29. Krestov GA (ed) (1995) Experimental methods of solution chemistry: spectroscopy and calorimetry. Nauka, Moscow (in Russian)
30. Kutepov AM (ed) (1997) Experimental methods of solution chemistry. Nauka, Moscow (in Russian)
31. Durov VA (2002) In: Concentrated and saturated solutions. Nauka, Moscow (in Russian), p 170
32. Burkert U, Allinger NL (1986) Molecular mechanics. Mir, Moscow (Russian translation)
33. Heerman DV (1990) Computer simulation methods in theoretical physics. Moscow (Russian translation)
34. Korolev GV, Ilyin AA, Solovyev NE, Mogilevich MM et al (2001) Vysokomolek Soedin A **43**:1822–1827 (in Russian)
35. Korolev GV, Ilyin AA, Solovyev NE, Mogilevich MM et al (2002) Vysokomolek Soedin A **44**:1947–1954 (in Russian)
36. Kargin VA, Kabanov VA, Papisov IM, Zubov VP (1961) Dokl Akad Nauk SSSR **141**:389–392 (in Russian)
37. Papisov IM, Kabanov VA, Kargin VA (1965) Vysokomolek Soedin **7**:1779–1785 (in Russian)
38. Kabanov VA, Papisov IM, Gvozdetskiy AN, Kargin VA (1965) Vysokomolek Soedin **7**: 1787–1791 (in Russian)
39. Korolev GV, Smirnov BR, Zhiltsova LZ et al (1967) Vysokomolek Soedin **9**:9–14 (in Russian)
40. Yong JS, Bowman CN (1999) Macromolecules **32**:6073–6081
41. Decker C (1998) Polym Int **45**:133–141
42. Tobita H (1998) Macromol Theory Simul **7**:225–232
43. Wen M, McCormick AV (2000) Macromolecules **33**:9247–9254
44. Okay O (1999) Polymer **40**:4117–4129
45. Denisov ET, Azatyan VV (1997) Inhibition of chain reactions. Institute of Chemical Phisics, Chernogolovka (in Russian)
46. Korolev GV (2003) Usp Khim **72**:222–244 (in Russian)

47. Denisov ET (1971) Liquid-phase reaction rate constants. Nauka, Moscow (in Russian)
48. Korolev GV (1965) Synopsis of thesis for doctor of science degree in chemistry. Institute of Chemical Physics of the USSR Academy of Science, Moscow (in Russian)
49. Golikov IV, Vasilyev DK, Mogilevich MM (1990) Izv Vuz Khim Khim Tekh **33**:94–99 (in Russian)
50. Vasiliyev DK, Belgovskiy IM, Mogilevich MM (1989) Vysokomolek Soedin A. **31**:1233–1237 (in Russian)
51. Lipatov YuS (1980) Interphase phenomena in polymers. Naukova Dumka, Kiev (in Russian)
52. Vasilyev DK, Golikov IV, Mogilevich MM et al (1987) Vysokomolek Soedin B **29**:563–564 (in Russian)
53. Brock T, Groteklaes M, Mischke P (2004) European coatings handbook: paint media. Moscow (Russian translation)
54. Mogilevich MM, Sukhanov GA, Korolev GV et al (1975) Vysokomolek Soedin A **17**:2390–2395 (in Russian)
55. Mogilevich MM, Sukhanov GA (1973) J LKM **2**:53–55 (in Russian)
56. Mogilevich MM, Sukhanova NA, Yablonskiy OM et al (1973) Izv Vuz Khim Khim Tekh **16**:1898–1903
57. Frank-Kamenetskiy DA (1966) Diffusion and mass transfer in chemical kinetics. Nauka, Moscow (in Russian)
58. Mogilevich MM (1979) Usp Khim **48**:362–386 (in Russian)
59. Mogilevich MM, Sukhanova NA, Korolev GV (1973) Vysokomolek Soedin A **15**:1478–1482 (in Russian)
60. Mogilevich MM, Sukhov VD, Yablonskiy OP et al (1977) Dokl Akad Nauk SSSR **232**:1355–1358 (in Russian)
61. Mogilevich MM, Krasnobaeva VS (1976) Izv Vuz Khim Khim Tekh **19**:105–108
62. Goodner MD, Bowman CN (1999) Macromolecules **32**:6552–6559
63. Elliot IE, Bowman CN (1999) Macromolecules **32**:8621–8628
64. Platkowski K, Reichert K-H (1999) Polymer **40**:1057–1066

http://www.springer.com/978-3-540-87566-6

Three-Dimensional Free-Radical Polymerization
Cross-Linked and Hyper-Branched Polymers
Korolyov, G.V.; Mogilevich, M.
2009, XVI, 272 p., Hardcover
ISBN: 978-3-540-87566-6